Biochemical and Phylogenetic Analysis of Organic Anion Transporting Polypeptides

A THESIS
SUBMITTED TO THE FACULTY OF
UNIVERSITY OF MINNESOTA
BY

Kayla Marie DeVoll

IN PARTIAL FULFILLMENT OF THE REQUIREMENTS
FOR THE DEGREE OF
MASTER OF SCIENCE

Jon N. Rumbley, Advisor

November, 2017

Acknowledgements

First, I would like to thank my family and friends, especially my parents, for all of their love, support and encouragement throughout my education. I would not have been able to do this without each and every one of you.

Second, I would like to thank my advisor, Dr. Jon Rumbley, for giving me this opportunity and shaping me into the scientist I am today. I will forever be grateful for this experience, even if it was the most challenging time of my life. I would also like to thank the members of my committee for all of the methodological advice, unique perspectives on my project and for reviewing my entire thesis. I especially want to thank Dr. Dan Westholm for all of the lab training because I couldn't be here without you!

Third, I would like to thank The College of Pharmacy faculty and staff for all of their help, guidance, and most importantly, all of the laughs.

And lastly, I would like to thank Doc Lach for all of the conversation and laughs, laboratory help, research advice and guidance, and helping to keep me sane through my graduate experience. Words cannot express how thankful I am to have you in my life.

Dedication

This thesis is dedicated to my grandfather, Earl Fagre. I know you would be proud of the person I have become.

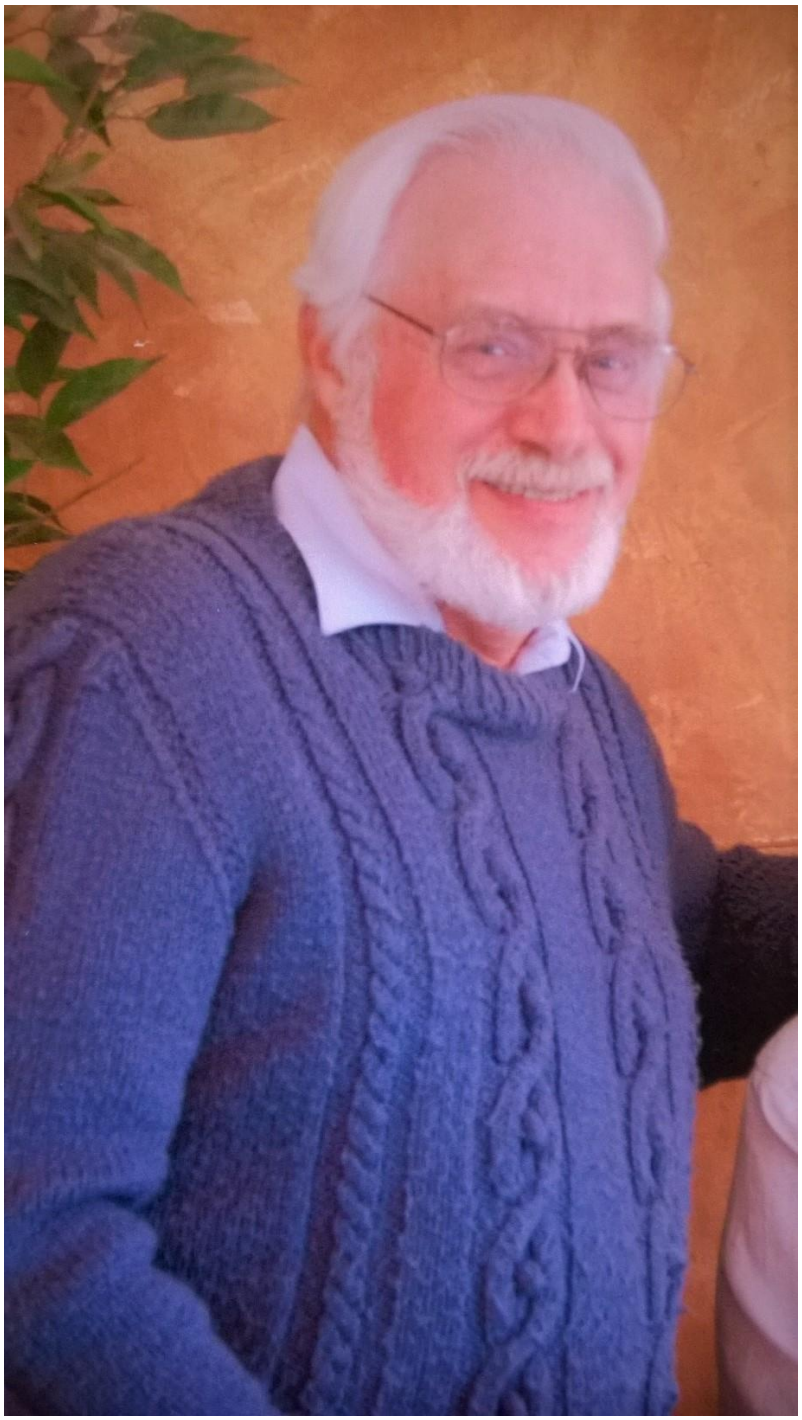

ABSTRACT

Organic Anion Transporting Polypeptides (Human: OATPs, all others: Oatps), are sodium-independent membrane transporters predicted to have 12-transmembrane domains. Oatps/OATPs mediate the transport of a broad range of endo- and xenobiotics including bile salts, hormones and their conjugates, statins, thyroid hormones, prostaglandins, and anticancer agents. Oatps have varying tissue expression profiles with some Oatps having a very discrete tissue-specific expression pattern while other Oatps are ubiquitously expressed throughout multiple tissues. The functional diversity displayed by Oatps/OATPs has made it difficult to understand their overall physiological role. The research presented here takes a two-pronged approach to elucidate the evolved physiological role of Oatps. The first approach investigates the active site structure of a specific Oatp, Oatp1c1, through transport inhibition and the second approach involves a comprehensive phylogenetic analysis of the Oatp family.

Oatp1c1 is expressed predominantly in the blood-brain barrier and the blood-cerebrospinal fluid barrier cells with minimal expression in specialized cells of the eye and gonads. Oatp1c1 has a narrower range of recognizable substrates compared to other Oatps. However, Oatp1c1 is a high affinity thyroxine transporter with the lowest K_m yet identified (10nM-340nM) of all transporters, indicating an important role in thyroid hormone homeostasis. Previous research suggests Oatp1c1 contains multiple binding sites based on the biphasic uptake curves of T4 and E_2-17β-G as well as T4 and E_2-17β-G *cis*-inhibition values differing from their K_ms. Unpublished data from the Rumbley Laboratory was used to characterize the Oatp1c1 T4 uptake site by calculating IC_{50}

values for multiple inhibitors of T4 uptake. However, the Oatp1c1 E_2-17β-G uptake site is not fully characterized.

In this study, HEK293 cells were transiently transfected with a Gateway expression vector, pEF-DEST 51, containing the Oatp1c1 gene sequence and uptake of ^{3}H-E_2-17β-G was assessed. Oatp1c1 expressing cells were found to uptake ^{3}H-E_2-17β-G 4-fold over empty vector transfected cells and uptake was shown in a time dependent manner. Next, multiple inhibitors were used to test their ability to inhibit the uptake of ^{3}H-E_2-17β-G and preliminary IC_{50} values were calculated and compared to the IC_{50} values calculated for the same inhibitors against the uptake of T4. Data presented here supports the idea of Oatp1c1 possessing a single flexible binding site capable of binding multiple substrate molecules simultaneously. However, the presence of multiple substrate binding sites capable of communication was not ruled out.

Oatps/OATPs are promiscuous membrane transporters and are highly conserved proteins present in all metazoans sequenced to date but are absent in all other organisms including plants, bacteria and yeast. Sequence alignments of *Homo sapiens* OATPs with that of primitive organisms have shown Oatps/OATPs have a high level of evolutionary conservation. Understanding why such primitive organisms like *Monosiga, Trichoplax* and *Nematostella* possess Oatps may allow clarification of the evolved physiological role of Oatps/OATPs. Due to the high level of Oatps/OATPs conservation among all metazoans, understanding the physiological purpose these transport proteins serve is important, especially since Oatps/OATPs are present in such a diverse range of organisms.

For comprehensive phylogenetic analysis of the Oatp family, *H. sapiens* OATP4A1 protein sequence was used as the query sequence for BLASTp searches completed against organisms with complete or nearly complete genomes. Multiple sequence alignments of all 1264 sequences were completed using MAFFT, QuickProbs and Clustal Omega. These alignments were compared to one another and subsequently submitted to FastTree 2.0 and MrBayes 3.2 for phylogenetic analysis. *Amphimedon queenslandica* was identified as the first metazoan to possess Oatp proteins and these protein sequences were more closely related to sequences within the Oatp4 family than to any other indicating the Oatp4 family was likely the first to evolve. Oatps/OATPs where shown to cluster into seven divergent families, with the seventh labeled as the Uncharacterized Oatp cluster. The Uncharacterized Oatp cluster emerges with the Bilaterian split of Protostomia and Deuterostomia but is lost somewhere in the chordate lineage before the emergence of vertebrates. Combined, both research studies will aid in the understanding of the evolved biological role of Oatps/OATPs and potentially lead to rational drug design of specifically targeted pharmaceutics.

Table of Contents

List of Tables

List of Figures

Chapter 1

Chapter 2

List of Abbreviations

3D	three dimensional
AHDS	Allan-Herndon-Dudley Syndrome
BBB	blood brain barrier
BCSFB	blood cerebrospinal fluid barrier
BLASTp	basic local alignment search tool
BSP	sulfobromophthalein
CNS	central nervous system
CoMFA	comparative molecular field analysis
CSF	cerebrospinal fluid
CYPs	cytochrome p450 enzymes
D2	iodothyronine deiodinase type 2
DHEAS	dehydroepiandosterone sulfate
E_2-17β-G	estradiol glucuronide
E-3-S	estrone-3-sulfate
ER	endoplasmic reticulum
EST	expressed sequence tags
HEK293	human embryonic kidney 293
MCT8	monocarboxylate transporter 8
MFS	major facilitator superfamily
MRP1	multidrug resistance-associated protein 1
NCBI	National Center for Biotechnology
Oatp/OATP	organic anion transporting polypeptide
rT3	reverse triiodothyronine or 3,3’,5’-triiodothyronine
SLC	solute carrier
T3	3,5,3’-triiodothyronine
T4	thyroxine
TM	transmembrane
TMD	transmembrane domain
UGTs	UDP-glucuronosyltransferase
UPGMA	unweighted pair group method with arithmetic mean
WAG	Whelan and Goldman

Chapter1

Inhibition of Organic anion transporting polypeptide 1c1-mediated uptake of Estradiol Glucuronide

INTRODUCTION

The central nervous system (CNS) is sealed from the exchangeable fluids of the body and passage into and from the CNS is tightly regulated to ensure proper functionality. This tight regulation is accomplished through the blood-brain barrier (BBB) and the blood-cerebrospinal fluid barrier (BCSFB). Due to the high metabolic demands of the brain, there is constant influx of nutrients and oxygen, along with an efflux of waste products [Takano et al., 2006]. This creates a necessity for both active and passive transport mechanisms within these barriers to ensure nutrient delivery into, and waste efflux out of, the CNS.

Blood-Brain Barrier

The BBB is selectively permeable and able to regulate the extracellular fluid of the CNS, independent of the peripheral circulation, in order to maintain CNS homeostasis [Wolka et al., 2003]. The BBB consists of microvascular endothelial cells along with an underlying basement membrane in which a number of pericytes are embedded at a rate of one pericyte per two endothelial cells, covering 99% of the capillary basement membrane [Engelhardt and Sorokin, 2009; Pardridge 2003]. The microvascular endothelial cells lack fenestrae causing minimal exchange between the blood and the CNS. This layer of microvascular endothelial cells and pericytes is ensheathed by astrocytic endfeet. The BBB is also characterized by a lack of paracellular diffusion between endothelial cells due to the presence of tight junctions which consist of claudin, occludin and junction adhesion molecule [Engelhardt and Sorokin, 2009; Wohlburg, 2002; Wolka et al., 2003]. Due to the lack of diffusion across the BBB, molecules must traverse both the luminal

and abluminal membranes of the capillary endothelium (separated by 100nm-300nm), as well as the pericyte and astrocytic endfeet [Pardridge, 2003]. With such an intricate cell-cell relationship as seen in the BBB, both active and passive transport systems are present to ensure the influx of nutrients and efflux of waste products into and out of the CNS.

Blood-Cerebrospinal Fluid Barrier

The BCSFB is made up of leaf-like, highly vascularized organs called choroid plexuses. Choroid plexuses are found in the roof of the third and fourth ventricles and the median walls of the lateral ventricles [Strazielle and Ghersi-Egea, 2000]. Each choroid plexus is comprised of a single layer of polarized cuboidal epithelial cells, called choroid plexus epithelial cells, which surround a vascular bed [Strazielle and Ghersi-Egea, 2000]. These vascular beds are fenestrated giving the basolateral membrane of choroid plexus epithelial cells direct access to blood contents. However, these epithelial cells are joined by apical tight junctions inhibiting the free diffusion of molecules from the blood into the cerebrospinal fluid (CSF). This allows the epithelial cells to tightly regulate the contents of CSF as molecules from the blood must traverse both the apical and the basolateral membranes in order to enter the CSF and visa-versa for molecules to exit the CSF and enter the blood circulation [Kusuhara and Sugiyama 2004; Strazielle and Ghersi-Egea 2000].

Introduction to Oatps/OATPS

One such transporter present within both the BBB and the BCSFB is Oatp1c1. Organic anion transporting polypeptides (Human: OATPs, all others: Oatps), are sodium-independent membrane transporters with 12 putative transmembrane domains (TMD)

which mediate the transport of a broad range of endo- and xenobiotics including bile salts, hormones and their conjugates, statins, thyroid hormones, prostaglandins, and anticancer agents. Based on sequence identity, Oatps/OATPs are grouped into families (>40% amino acid sequence identity) and subfamilies (>60% amino acid sequence identity) with human and rodent Oatps/OATPs forming six families (OATP1-OATP6) and thirteen subfamilies (OATP1A-OATP6D) [Hagenbuch and Meier, 2003]. Oatps/OATPs have varying tissue expression profiles with some Oatps/OATPs demonstrating discrete tissue-specific expression while other Oatps/OATPs demonstrate ubiquitous expression and are found in almost all tissues (Fig. 1). For example, OATP1B1 and OATP1B3 are exclusively expressed at the sinusoidal membrane of hepatocytes and exhibit a wide range of recognizable substrates (Fig. 1) [König et al., 2000; Roth et al., 2012; Tamai et al., 2000]. On the other hand, OATP3A1 and OATP4A1 are ubiquitously expressed throughout the body as evidenced by their mRNA present in almost all tissues analyzed and have a more limited substrate profile compared to the OATP1 family (Fig. 1) [Adachi et al., 2003; Fujiwara et al., 2001; Huber et al., 2007; Tamai et al., 2000].

Oatp1c1/OATP1C1

Oatp1c1 is exclusively expressed at blood-tissue barriers, with the majority of the protein expressed within the CNS and found in both the BBB and the BCSFB [Gao et al., 2005; Pizagalli et al., 2002; Roberts et al., 2008; Schnell et al., 2015; Sugiyama et al., 2003b; Tohyama et al., 2004]. Oatp1c1 is enriched in brain microvessel endothelial cells compared to whole brain, is expressed along both the abluminal and

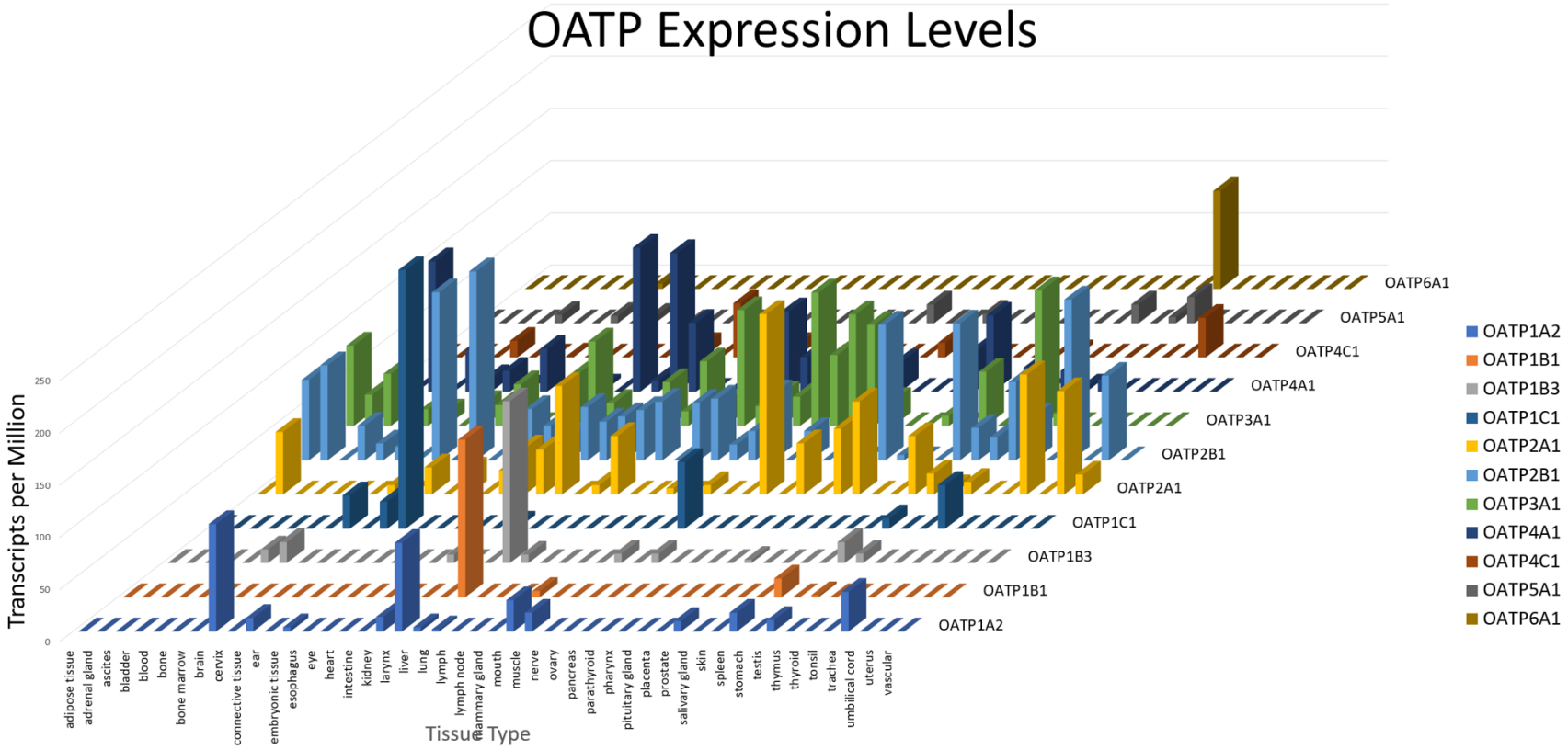

Figure 1. OATP Tissue Expression Profiles. OATPs display varying tissue expression profiles within humans. Expressed sequence tag (EST) data for each OATP, displayed in transcripts per million, shows its level of expression within each tissue type. EST data displayed is from NCBI UniGene website (https://www.ncbi.nlm.nih.gov/unigene).

luminal membranes of the BBB, and is also present in astroglial endfeet [Müller and Heuer, 2014; Roberts et al., 2008; Schnell et al., 2013; Sugiyama et al., 2003b]. Within the BCSFB, Oatp1c1 is expressed along both the apical and basal membranes as well as tanycytes of the third ventricle [Roberts et al., 2008; Tohyama et al., 2004]. Oatp1c1 shows minimal expression within Leydig cells of the gonads as well as the abluminal and luminal membranes of the retinal capillaries and the basolateral membrane of rat retinal pigment epithelial cells [Akanuma et al., 2013; Pizzagalli et al., 2002].

OATP1C1 is expressed within the CNS, however the expression of Oatp1c1 was not enriched in brain microvessel endothelial cells compared to whole brain [Roberts et al., 2008]. OATP1C1 demonstrates a scattered expression pattern throughout adult and fetal brain showing expression in microvessels of the BBB, both the apical and basal membranes of the BCSFB, and glial cells throughout the hypothalamus and wall of the third ventricle [Alkemade et al., 2011; Roberts et al., 2008].

Oatp1c1 has a narrower range of recognizable substrates compared to other Oatps. However, Oatp1c1 is a high affinity thyroxine (T4) transporter with the lowest K_m yet identified (10nM-340nM) of all Oatp/OATP transporters [Pizzagalli et al., 2002; Sugiyama et al., 2003b; Tohyama et al., 2004; Westholm et al., 2009a]. Oatp1c1 also transports estradiol-17β-glucuronide (E_2-17β-G) but with a lower affinity compared to T4, with a reported K_m between 10μM-23.5μM [Sugiyama et al., 2003b; Tohyama et al., 2004; Westholm et al., 2009a]. Other Oatp1c1 substrates include 3,3',5'-triiodothyronine (rT3), 3,5,3'-triiodothyronine (T3), sulfobromophthalein (BSP), and estrone-3-sulfate (E-3-S) [Pizzagali et al., 2002; Sugiyama et al., 2003b; Tohyama et al., 2004].

Characterization of Oatps/OATPs is incomplete with few kinetic constants (V_{max} and K_m) known for Oatp/OATP substrates. Elucidation of kinetic constants for substrates allows for a clearer picture of the enzymes contribution to *in vivo* metabolism of drugs and their overall clearance rates. Typically, Michaelis-Menten kinetics are used to describe substrate metabolism while operating under a number of assumptions including the enzyme having only one binding site [Tracy and Hummel, 2004]. However, many Oatps/OATPs may contain more than one binding site because they can accommodate multiple different substrates. Also, *cis*-inhibition studies using multiple substrates result in an unequal K_m and K_i for each substrate. For example, previous research demonstrated the *cis*-inhibition of Oatp1c1 uptake of T4 and E_2-17β-G resulted in unequal K_i and K_m values for each substrate, leading to the conclusion Oatp1c1 contains two substrate recognition sites [Tohyama et al., 2004]. Recently, research suggested Oatp1c1 mediated uptake of T4 and E_2-17β-G was biphasic, again with substrates K_i and K_m values unequal, further adding evidence to Oatp1c1 having two substrate recognition sites [Westholm et al., 2009a]. Also, OATP4C1 is thought to contain multiple binding sites evidenced by the unequal K_m and IC_{50} values for digoxin against E-3-S uptake [Yamaguchi et al., 2010].

With growing evidence of Oatps/OATPs containing more than one binding site it is clear Michaelis-Menten kinetic models will not give the most accurate depiction of substrate metabolism. Instead, a biphasic kinetic profile has been used to describe the substrate metabolism of multiple Oatps/OATPs including Oatp1a4, OATP1B1, OATP1B3, Oatp1c1 and OATP2B1 [Gui et al., 2008; Sugiyama et al., 2002; Tamai et al.,

2001; Tohyama et al., 2004; Westholm et al., 2009a]. The use of the correct kinetic model is important for accurately estimating kinetic constants for an enzyme as the use of an incorrect model could cause miss-estimation of drug clearance *in vivo* and *in vitro*. This is important for determining potential drug-drug interactions *in vivo*.

OATP Expression at the BBB & BCSFB

To date, more than 300 members of the Oatp/OATP superfamily are either identified or predicted in more than 40 different species [Hagenbuch and Steiger, 2013]. Of these, only six are identified on the protein level and found expressed within the BBB and/or the BCSFB within mammals including OATP1A2, Oatp1a4, Oatp1a5, Oatp1c1, OATP1C1, and OATP3A1 [Alkermade et al., 2011; Gao et al., 1999 and 2000; Huber et al., 2007; Kushuhara et al., 2002; Muller and Heuer, 2014; Ohtsuki et al., 2004; Roberts et al., 2008; Schnell et al., 2013; Sugiyama et al., 2003; Tohyama et al., 2004]. Most of these Oatps/OATPs are asymmetrically expressed within the polarized cell barriers of the BBB and the BCSFB. Some Oatps/OATPs are only expressed on one cell membrane (abluminal vs. luminal or apical vs. basolateral) of the BBB or BCSFB but other Oatps/OATPs are expressed on both membranes. For example, OATP3A1, having two splice variants labeled OATP3A1_v1 and OATP3A1_v2, is found on both membranes of BCSFB with OATP3A1_v1 expressed on the basolateral membrane of the choroid plexus while OATP3A1_v2 is expressed along the apical membrane [Huber et al., 2007]. Some Oatps/OATPs may also show differential expression depending on the tissue they are expressed in. For example, Oatp1a4 is expressed at the luminal and abluminal membranes of capillary endothelial cells but only located on the basolateral membrane of

the choroid plexus [Gao et al., 1999].

The function of the BBB and the BCSFB is to transport essential compounds and metabolites to maintain homeostasis of the CNS and to limit uptake of xenobiotics. These solutes must pass both the luminal and abluminal membranes of capillary endothelial cells, which are separated by 100nM-300nM, as well as the pericytes and astrocytes in order to enter the CNS [Pardridge, 2003]. Or, in the case of the BCSFB, solutes must traverse both the apical and basolateral membranes of the choroid plexus epithelial cells to enter or exit the CSF. The advantage of asymmetric distribution of these Oatps/OATPs is to make more compounds available for exchange within the CNS and to concentrate solutes within either the plasma or the brain parenchyma [Drewes, 2000]. This can allow for the directional transport and/or excretion of compounds from the brain and prevent accumulation of substrates within the CNS.

The BBB and the BCSFB form a metabolic barrier protecting the brain from harmful endobiotics and xenobiotics. Oatps/OATPs are likely to play a major role in this process due to their asymmetric expression within both the BBB and the BCSFB and by their polarized transport of conjugated metabolites. Oatp1a4, Oatp1a5 and Oatp1c1 are asymmetrically expressed within these tissues with Oatp1c1 and Oatp1a5 expressed at the apical membrane of the BCSFB and Oatp1a4 and Oatp1c1 expressed on the basolateral membrane [Gao et al., 1999; Kusuhara et al., 2002; Ohtsuki et al., 2004; Roberts et al., 2008; Sugiyama et al., 2003b; Tohyama et al., 2004;]. In the BBB, Oatp1a4, Oatp1a5 and Oatp1c1 are expressed on both the luminal and abluminal membranes [Gao et al., 1999; Kusuhara et al., 2002; Ohtsuki et al., 2004; Roberts et al.,

2008; Sugiyama et al., 2003b].

Substrate Metabolism at the BBB and BCSFB

Tight regulation of the CNS is accomplished through the BBB and the BCSFB. One role these barriers play in regulating the CNS is through the detoxification of xenobiotics and the metabolism of endobiotics accomplished through the expression of membrane transporters and metabolic enzymes in barrier cells. This allows for protection against hazardous substances and helps to regulate the activities of endogenous substrates. This means Oatps/OATPs expressed in the membranes of the BBB and the BCSFB cooperate with metabolic enzymes expressed within these barrier cells to tightly regulate the levels of endo- and xenobiotics within the brain.

There are three types of reactions involved in the metabolism of endo- and xenobiotics including oxidative reactions, conjugations reactions, and transport metabolism. Oxidative metabolism involves the addition of a new functional group, modification to an already existing functional group, or hydrolysis to expose a site for conjugation. All of these reactions occur via the Cytochrome P450 enzymes (CYPs) present along the membrane of endoplasmic reticulum (ER). In the case of E_2-17β-G specifically, cholesterol first undergoes oxidative metabolic reactions by CYP19 to eventually become estradiol. CYP19 is also widely expressed in mammalian brain [Hedlund et al., 2001].

Conjugation reactions involve the addition of a new charged group to the endo- or xenobiotic molecule in order to mask an already existing functional group. This further increases the polarity of the substrate making it nearly impossible to diffuse across the

plasma membrane and marks the substrate for elimination from the body. For glucuronidation, which estradiol undergoes to become E_2-17β-G, the active form of glucuronic acid, or uridine diphosphate glucuronic acid, is added to an existing functional group on the substrate by a UDP-glucuronosyltransferase (UGTs). UGTs are located along the luminal side of the ER membrane. Three isoforms of UGTs are expressed within the brain including UGT1A6, 2A1 and 2B7. UGT1A6 is localized to tissues of the liver, kidney and brain in humans but was not found in brain microvessels [King et al., 1999; Shawahna et al., 2011]. UGT2A1 was found in total brain and in olfactory epithelium suggesting UGT2A1 plays a role in odorant signaling [Jedlitschky et al., 1999; King et al., 2000]. UGT2B7 is localized to tissues of the liver, kidney and pancreas, and found in human cerebellum [King et al., 1999].

After oxidative and conjugation metabolism have taken place, the endo- or xenobiotic is considerably more polar making membrane transporters important for elimination of the endo- or xenobiotic from tissues. Oatps/OATPs are present on the BBB and the BCSFB and known to transport conjugated endo- and xenobiotics making them important facilitators of transport metabolism. Because Oatps/OATPs are present on both membranes of the BBB and the BCSFB, they likely participate in both the influx and efflux of conjugated metabolites. For the BCSFB, choroid plexus epithelial cells are responsible for the detoxification of CSF through the metabolism of endobiotics and xenobiotics. This is evidenced by the uptake of 1-naphthol into choroid plexus epithelial cells and the polarized elimination of 1-naphthyl-β-D-glucuronide through the basolateral membrane [Straziielle and Ghersi-Egea, 1999].

E_2-17β-G is shown to be rapidly eliminated from CSF after intracerebroventricular injection with Oatp1a5 responsible for a majority of the uptake into the choroid plexus epithelial cell along the brushborder membrane [Kusuhara et al., 2003; Lee et al., 2004; Nishino et al., 1999]. Oatp1c1 is also expressed along the brushborder membrane of the choroid plexus and E_2-17β-G is a known substrate. So, Oatp1c1 could also be partially responsible for E_2-17β-G elimination from the CSF. It is, however, unclear what transporter(s) is responsible for the elimination of E_2-17β-G from the choroid plexus epithelial cells along the basolateral membrane. Multidrug resistance-associated protein 1 (Mrp1) is expressed along the basolateral membrane and is known to transport E_2-17β-G [Nishino et al., 1999; Rao et al., 1999]. However, the E_2-17β-G elimination rate from CSF was not significantly different between wildtype and Mrp1 gene knockout mice indicating a minimal role for Mrp1 in E_2-17β-G efflux from the CSF [Lee et al., 2004]. Mrp1 is also expressed along the luminal membrane of the BBB and E_2-17β-G elimination from the brain across the BBB after microinjection was significantly decreased in Mrp1 gene knockout mice [Sugiyama et al., 2001; Sugiyama et al., 2003a]. Oatp1a4 is responsible for 40% of E_2-17β-G elimination across the BBB indicating Oatp1a4 works in conjunction with Mrp1 to eliminate E_2-17β-G from the brain across the BBB [Sugiyama et al., 2001]. Oatp1c1 is also expressed along the luminal membrane of the BBB suggesting a role in E_2-17β-G elimination.

Thyroid Hormone Action in the CNS

Thyroid hormones are dependent upon membrane transporters present in both membranes of the BBB and BCSFB in order to cross these barrier cells and enter the

CNS [Heuer, 2007]. Thyroid hormone plays a critical role during the developmental stages of mammalian brain. T4 is a prohormone and is the main product secreted by the follicular cells of the thyroid gland [Friesema et al., 2005]. Iodothyronine deiodinases, specifically type two deiodinases (D2), are responsible for the removal of a 5' outer ring iodine from T4 creating T3. T3 is the active form of thyroid hormone and works by binding to the nuclear thyroid hormone receptors altering downstream gene expression [Friesema et al., 2005].

The early stages of mammalian brain development is marked by neuronal histogenesis and migration followed by maturation, dendritic growth, synapse formation and myelination [Anderson et al., 2003]. Absence of thyroid hormones or abnormal thyroid hormone levels during brain development can cause intellectual impairments as evidenced in Allan-Herndon-Dudley syndrome (AHDS) [Anderson et al., 2003, Stevenson et al., 1990]. AHDS is characterized by severe psychomotor retardation and abnormal thyroid hormone parameters with elevated serum T3 and lowered serum T4 levels [Maranduba et al., 2006]. Mutations to monocarboxylate transporter 8 (MCT8), a thyroid hormone transporter, is the cause of AHDS [Friesema et al., 2004].

In humans, MCT8 is enriched in brain microvessels in the cerebral cortex and the hippocampus with expression on both the apical and basal membranes of the BCSFB [Roberts et al., 2008]. MCT8 transports both T3 and T4 but functional analysis of transfected cells demonstrated a preferential transport of T3 by MCT8 [Friesema et al., 2006; Maranduba et al., 2006]. Because MCT8 expression is enriched along the BBB in humans, MCT8 is likely responsible for the majority of thyroid hormone uptake into the

brain across the BBB [Roberts et al., 2008]. OATP1C1 is expressed along the BBB but not at the same intensity as MCT8. Therefore, OATP1C1 is likely responsible for the transport of T4 out of microvessel endothelial cells and the subsequent influx into glial cells [Roberts et al., 2008]. Within glial cells, T4 is converted to active T3 by D2, consistent with data showing a majority of T3 is created locally in rat cerebral cortex [Crantz et al., 1982]. From here, T3 is transported into the adjacent neuron via MCT8 where T3 binds to the nuclear receptor [Schweizer and Köhrle, 2013]. However, MCT8 knockout mice fail to show any neurological symptoms but MCT8/Oatp1c1 double knockout mice exhibited delayed cerebellar development [Mayerl et al., 2014; Trajkovic et al., 2007]. This is likely due to the enriched expression of Oatp1c1 in the BBB of mice. Therefore, OATP1C1 expression in human microvessels may not be adequate to compensate for the loss of function of MCT8 in AHDS afflicted patients [Roberts et al., 2008]. However, studies show interindividual variation of OATP1C1 expression levels within human brain so the exact mechanism or contribution of OATP1C1 to thyroid hormone levels in AHDS patients is unclear [Roberts et al., 2008].

OATP Transport Mechanism

Oatps/OATPs are members of the Major Facilitator Superfamily (MFS) of proteins. The MFS makes up the largest family of secondary active transporters. Evidence suggests all members of the MFS share the same three-dimensional (3D) structure, called the MFS fold, consisting of 12 TMD that are organized into two discrete domains, N-terminal domain and C-terminal domain, making a 2-fold symmetry with an axis perpendicular to the membrane.

Sequence analysis of some MFS proteins suggests a duplicated 3 transmembrane (TM) helices repeat within each domain giving the corresponding helices within each of these domains the same general structure and position within the membrane [Abramson et al., 2003; Huang et al., 2003; Hvorup and Saier, 2002; Yin et al., 2006]. Within the center of the transporter are TM helices 1, 4, 7 and 10, with these helices mainly responsible for substrate binding and transport. Helices 2, 5, 8 and 11 are located on the sides of the structures mediating contact areas and may also participate in substrate binding. This leaves helices 3, 6, 9 and 12 located on the outside of the structure, interacting with the membrane and maintaining protein structure.

Homology modeling has been used to form a 3D structure and transport mechanism of Oatps/OATPs due to the lack of an existing crystal structure. Crystal structures of three prokaryotic antiporters within the MFS family are available and these antiporters share high sequence similarities with Oatps/OATPs and were subsequently used to form this 3D model. This includes the glycerol-3-phosphate transporter, lactose permease and the multidrug transporter in *E. coli*. The elucidation of these crystal structures indicated a rocker-switch type mechanism was the fundamental mode of substrate transport [Law et al., 2008; Meier-Abt et al., 2005].

The rocker-switch transport mechanism involves the N- and C-terminal domains of the protein rocking back and forth against each other allowing the substrate to gain access to the other side of the membrane [Huang et al., 2003; Law et al., 2008; Meier-Abt et al., 2005]. In the case of the glycerol-3-phosphate transporter in *E. coli*, the active site is composed of arginine residues on helices 1 and 7 of the N- and C-terminals, respectively

[Huang et al. 2003]. Upon substrate binding to the active site, the two arginine residues are pulled closer together and this subsequently, pulls the N- and C-terminal domains together [Huang et al. 2003]. The tilting of these domains relative to each other causes the central pore to close on the cytosolic side and opens the pore to the extracellular side [Huang et al. 2003]. Substrate binding is thought to lower the energy barrier between the two conformations of the protein allowing the change from intracellular to extracellular facing [Huang et al. 2003]. Because Oatps/OATPs are part of the MFS family and share sequence homology with these transporters in *E. coli*, they likely utilize the same transport mechanism and have the same overall topology.

Research suggests Oatps/OATPs are anion exchangers. This means substrate accumulation within the cell is driven by the free energy created from transporting a counter ion down the ion's gradient. An outwardly directed pH gradient; the pH is greater inside the cell vs. outside the cell; resulted in a two-fold increase in taurocholate transport by rat Oatp1a1 over an inwardly directed pH gradient [Satlin et al. 1997]. This indicates the import of substrates by Oatps/OATPs is coupled to the export of OH- or HCO_3- anions and transport is dependent upon pH [Satlin et al. 1997]. Reduced glutathione and glutathione conjugates also act as counter ions for some Oatps/OATPs. Taurocholate and leukotriene C4 transport via rat Oatp1a1 was trans-stimulated by glutathione [Li et al. 1998]. Taurocholate transport via rat Oatp1a4 was also trans-stimulated by glutathione conjugates but not rat Oatp1a1 [Li et al. 2000]. This indicates not all Oatps/OATPs operate by the same overall driving force.

Using Oatps/OATPs close relation to multiple MFS proteins, Meier-Abt et al.

demonstrated *in silico* OATP1B3 has a central twofold symmetry axis perpendicular to the cell membrane and also possesses a central pore open to the intracellular side [Meier-Abt et al. 2005]. This symmetry axis is surrounded by the six N-terminal helices and the six C-terminal helices with helices 1, 2, 4, and 5 of the N-terminal half and helices 7, 8, 10 and 11 of the C-terminal half facing the central pore leaving helices 3, 6, 9 and 12 embedded within the cell membrane [Meier-Abt et al. 2005]. This model of OATP1B3 demonstrated a positive electrostatic potential within the central pore consistent with the majority of Oatps/OATPs substrates being anionic compounds [Meier-Abt et al. 2005]. Also, the outer surface of the protein has a neutral potential consistent with being an integral-membrane protein [Meier-Abt et al. 2005].

Structural Characteristics

Since no crystal structure yet exists for Oatps/OATPs, most structural analysis is completed using hydropathy analysis. From this type of analysis, Oatps/OATPs are predicted to have 12 TMD with both the N-terminus and C-terminus on the cytosolic side [Hagenbuch and Meier, 2003]. Multiple N-glycosylation sites are present in extracellular loops 2 and 5 which are also conserved among most Oatps/OATP families and needed for proper membrane localization [Hagenbuch and Meier 2004; Lee et al. 2003].

OATPs have a large 5th extracellular loop containing ten highly-conserved cysteine residues [Hagenbuch and Meier, 2003]. Mutational analysis of OATP2B1 conducted by Hänggi et al. revealed all cysteine residues are disulfide bonded and all cysteine residues, except for C493 and C557, are essential for membrane expression and proper functionality [Hänggi et al. 2006].

The 13-amino acid Oatp/OATP superfamily consensus sequence on extracellular loop 3 and TMD 6 is highly conserved and has been used to identify Oatps present in other species [Hagenbuch and Meier, 2003]. The consensus sequence contains three conserved tryptophan residues and it is still unknown whether this sequence serves any functional purpose.

Oatp1c1 Substrate Structural Features

Molecules unable to freely diffuse across the plasma membrane rely of specific membrane transporters expressed within the BBB and the BCSFB to enter or exit the CNS. The active site of these membrane transporters likely contains a molecular surface complimentary to the substrates surface. For example, where the substrate has a hydrogen bond donor the proteins active site would have a hydrogen bond acceptor. With considerable overlap between the recognizable substrates of Oatps/OATPs and the lack of any Oatp/OATP 3D structures, knowledge is gained from analyzing the common chemical features of transported substrates and can aid in the development of specifically targeted pharmaceuticals.

Yarim et al. performed comparative molecular field analysis (CoMFA) on 18 substrates transported by Oatp1a5 resulting in a topological model of the substrate binding site within Oatp1a5 [Yarim et al., 2005]. Three important chemical features where found conserved between all 18 substrates analyzed including a negatively charged group, a hydrogen bond donor and an extended hydrophobic region [Yarim et al., 2005]. Substrates exhibiting all of these features likely have a higher binding affinity with Oatp1a5 than substrates that have only one or two. However, the 3D positioning of each

of these features within the substrate is vital to the substrates ability to effectively bind the active site of the protein. Substrates such as E-3-S and dehydroepiandrosterone sulfate (DHEAS), possessing negatively charged sulfate groups where the CoMFA model exhibited a positive charge, had some of the lowest affinities out of all substrates tested [Yarim et al., 2005].

A similar analysis was completed by Chang et al. on Oatp1a1 and OATP1B1 by generating pharmacophores for both transporters gaining structural insights into the molecular features of each transporters substrates [Chang et al., 2005]. The resulting meta-pharmacophore built for both transporters contained two hydrogen bond acceptors located on opposite ends of the molecule and three hydrophobic areas located between the two hydrogen bond acceptors [Chang et al., 2005]. Although, these chemical features have varying 3D positions within the substrates depending on the transporter as evidenced by DHEAS having medium affinity for Oatp1a1 and low affinity for OATP1B1 due to its failure to occupy a hydrophobic and hydrogen bond acceptor feature [Chang et al.,2005].

The results of both Yarim et al. and Chang et al. demonstrate multiple Oatps/OATPs prefer similar chemical features in their substrates. The analysis of substrates for Oatp1a5, Oatp1a1 and OATP1B1 indicate each transporter has a higher affinity for substrates with hydrogen bond acceptors, or polar groups, located on each end of the molecule with an extended hydrophobic area in between [Chang et al., 2005; Yarim et al., 2005]. Based on this evidence, the active sites of Oatps/OATPs likely contain similar chemical structures in order to accommodate many of the same substrates

albeit with different affinities. By creating models *in silico* of OATP1B3 and OATP2B1, Meier-Abt et al. demonstrated the putative pores have positive electrostatic potential consistent with Oatps/OATPs ability to bind and translocate anionic compounds [Meier-Abt et al., 2005].

Since Oatp1c1 is solely expressed at the BBB and BCSFB, the number of substrates recognized by Oatp1c1 is not surprisingly limited compared to other Oatps/OATPs. Even with this in mind the chemical features of thyroxine agree with the CoMFA analysis completed for Oatp1a5 by Yarim et al. [Yarim et al., 2005]. However, comprehensive CoMFA type studies remain incomplete for Oatp1c1/OATP1C1 so conclusions about substrate commonalities cannot be drawn yet.

In order to determine if Oatp1c1 possesses a single flexible binding site or multiple binding sites, uptake of E_2-17β-G by empty vector and Oatp1c1 transfected cells was measured in both the absence and presence of multiple different inhibitors. Uptake of E_2-17β-G by Oatp1c1 transiently transfected cells was 4-fold over empty vector transfected cells. Nine different inhibitors were used against the uptake of E_2-17β-G and their preliminary IC_{50} values calculated. The preliminary IC_{50} values for each inhibitor were compared to IC_{50} values for the same inhibitor against the Oatp1c1-mediated uptake of T4 and used to determine if the active site of Oatp1c1 is a single, large flexible substrate binding site or if the active site is made up of multiple substrate binding sites.

MATERIALS AND METHODS

Transient Transfections

HEK293 cells were plated at $2.5x10^5$ cells per well in a 4-well plate coated with rat tail collagen (BD Biosciences) in complete MEM containing FBS (10% v/v), sodium pyruvate (10mM), non-essential amino acids (1x), and penicillin-streptomycin (1%). Plates were incubated for 24 hours at 37°C with 5% CO_2 to reach 90% confluence before media was changed to Opti-MEM supplemented with FBS (10% v/v), sodium pyruvate (10mM) and non-essential amino acids (1X). For the transfections, 1.0 µg of plasmid DNA was diluted into 50µl Opti-MEM along with 2µL P3000 Reagent. Lipofectamine 3000 (1.5µL) was diluted into 50µL of Opti-MEM and mixed with 50µL of the Opti-MEM and DNA mixture. The solution was incubated for 5 minutes at room temperature before 50µL was added to each well. Plates were incubated at 37°C with 5% CO_2 for 4 hours before the media was changed to MEM containing stripped FBS (10% v/v), sodium pyruvate (10mM), sodium butyrate (10mM) and non-essential amino acids (1X).

Total mRNA Isolation and PCR

Total mRNA was isolated from transiently transfected cells expressing Oatp1c1, pEF-DEST 51 vector alone, and untransfected HEK293 cells using Qiagen RNeasy Mini kit (Cat. No. 74104). cDNA synthesis was completed using 5µg of total mRNA utilizing random hexamers according to the product manual (Invitrogen, Cat. No. 18080-051). Forward and reverse sequence specific primers were designed.

Oatp1c1 forward: 5' TCG-CAG-TTC-CCC-AGT-TCT-TC 3'

Oatp1c1 reverse: 5' GTT-GGG-AGT-GAG-GTT-GGA-GG 3'

V5/6x His forward: 5’ GTG-GTT-GAT-CTA-GGC-CC 3’

V5/6x His reverse: 5’ TGA-TGG-TGA-TGA-TGA-CCG-GTA-CG 3’

Thermocycler settings consisted of the following: Step 1: 94ºC for 30s, Step 2: (35x) 94ºC for 15s, 53ºC for 30s, 68ºC for 1:30min, Step 3: 68ºC for 5min, Step 4: hold at 4ºC.

Transport Assays

Cells were plated at 2.5 $x10^5$ cells per well in 4-well plates coated with rat tail collagen (BD Biosciences) in complete media. Twenty-four hours prior to assay, media was changed to complete media supplemented with stripped-FBS (10% v/v), non-essential amino acids (1X), sodium pyruvate (10mM) and sodium butyrate (10mM). Stripped serum was prepared by incubating 50mLs FBS with 2.5g Dowex 1x8, 50-100 mesh, ion-exchange resin (Sigma-Aldrich) three times for 2 hours each at room temperature. After final incubation, serum was centrifuged at 3500xg to pellet beads and filter sterilized. To perform the assay, cells were washed twice and incubated at 37ºC with 0.5mLs of pre-warmed Krebs-Henseleit buffer [142mM NaCl, 23.8mM $NaHCO_3$, 12.5mM HEPES, 5mM glucose, 4.83mM KCl, 1.53mM $CaCl_2$, 1.2mM $MgSO_4$, and 0.96mM KH_2PO_4 (pH 7.4)]. Uptake was initiated with the addition of 200µL of Krebs-Henseleit containing 55nM ^3H-E_2-17β-G (specific activity 41-50 Ci/mmol; PerkinElmer). Cells were lysed with 1% Triton X-100 in PBS and associated radioactivity measured using a Beckman LS-6500 Scintillation Counter. Protein concentrations were determined using a bicinchoninic assay kit (ThermoFisher Scientific). Uptake was calculated from the proportion of radioactivity in each cell lysate compared to the total radioactivity associated with the isotopic Krebs-Henseleit buffer. Uptake was expressed in units of

picomoles per minuter per milligram of protein.

Immunohistochemistry

Transiently transfected HEK293 cells were plated in 24-well plates containing 12mm round cover slips coated with poly-L-lysine (BD Biosciences). Cells were rinsed with room temperature 1X PBS, followed by room temperature methanol, then fixed in methanol at -20^{o}C for 24hrs. Next, cells were washed, permeabilized, and blocked during three 5-min washes in PBS, 1% BSA, 0.1% Triton X-100. Anti-V5-FITC antibody (Invitrogen; R963-25), at a 1:350 dilution, was applied to the coverslips, along with 0.5µg/mL of Hoechst stain, for 1 hour in a humidity chamber placed in a 37^{o}C incubator. After incubation, cells received three 5-min washes in 1X PBS and were mounted using a Prolong Anti-Fade kit (Invitrogen).

Time Course

Uptake of 55nM ^{3}H-E_2-17β-G was examined at various time points from 30sec to 30 min. Background radioactivity associated with a blank sample of 1% Triton X-100 was subtracted from all samples.

Dose Response

Uptake of 55nM ^{3}H-E_2-17β-G in the presence of various inhibitor concentrations was measured after 4min of incubation at 37^{o}C. Substrate and inhibitor cocktails were mixed just prior to assay and kept in the dark until needed.

RESULTS

Expression of Oatp1c1 in HEK293 cells

The Oatp1c1 gene sequence was previously inserted into the Gateway expression vector pEF-DEST 51 and sequence verified [Westholm et al., 2009a]. Immunohistochemistry and PCR were performed to verify expression in transfected HEK293 cells. Immunohistochemistry of untransfected, empty vector and Oatp1c1 transiently transfected HEK293 cells was completed using an anti-V5-FITC conjugated antibody. Very minimal staining was seen in the untransfected and empty vector transfected HEK293 cells (Fig. 1A-B). Staining of the Oatp1c1 transiently transfected cells revealed cellular membrane localization (Fig. 1C). Some cells also had Oatp1c1 localization on the endoplasmic reticulum (data not shown) consistent with previous findings [Westholm et al., 2009a].

Total mRNA was isolated from untransfected, empty vector and Oatp1c1 transfected HEK293 cells and reverse transcribed into cDNA. PCR was performed using sequence specific primers designed to give a product spanning the protein-epitope tag fusion junction (Fig. 2A-B). As expected, no bands were visible in lanes 1 and 2 (Fig. 2A) containing cDNA from untransfected cells. Lane 3, containing cDNA from empty vector transfected cells, also had no visible band (Fig. 2A). The band expected in the Oatp1c1 PCR reaction using Oatp1c1 sequence specific forward primer and the V5/6xHis reverse primer was 1835 base pairs and is visible in lane 4 (Fig. 2A). This indicates the Oatp1c1 gene is expressed post-transfection in HEK293 cells.

Oatp1c1-dependent ^{3}H-E$_2$-17β-G uptake

Uptake of 55nM ^{3}H-E$_2$-17β-G by empty vector and Oatp1c1 transfected HEK293 cells was measured over the course of 30 minutes at 37^{o}C (Fig. 3). Radioactivity levels associated with a blank sample of 1% Triton X-100 in PBS was subtracted from all samples. Oatp1c1-mediated uptake of ^{3}H-E$_2$-17β-G was time dependent and 4-fold higher than empty vector transfected cells. The data was fit using a two-phase association equation, modeling uptake as the sum of two components: a fast (K_{fast}) and a slow (K_{slow}). This equation offered the best R^2 value of 0.8866. Fitting the data using a one phase association model, which describes the kinetics of the interaction between a substrate and an enzyme, had an R^2 value of 0.7680. With such a large difference in R^2 values it seems likely Oatp1c1 has two substrate binding sites instead of one. This data is in consensus with previous research indicating Oatp1c1 displays biphasic uptake kinetics [Tohyama et al., 2004; Westholm et al., 2009a].

Inhibition of Oatp1c1-mediated ^{3}H-E$_2$-17β-G transport

Previous dose response experiments using multiple inhibitors against the Oatp1c1-mediated uptake of ^{125}I-T4 have already been completed by the Rumbley Laboratory. A subset of these same inhibitors was used to test the inhibition of Oatp1c1-mediated uptake of ^{3}H-E$_2$-17β-G. The structure of ^{3}H-E$_2$-17β-G and all inhibitors used are shown in Figure 4. Preliminary dose-response analysis was completed for taurocholate, pravastatin, meclofenamic acid, T4, WY-14643, 4-hydroxytamoxifen, diclofenac sodium salt, estrone-3-sulfate and BSP (Fig. 5). Oatp1c1-mediated uptake of 55nM ^{3}H-E$_2$-17β-G was measured at four minutes of incubation at 37^{o}C in the presence of increasing

concentrations of each inhibitor. The uptake of ^{3}H-E_2-17β-G into empty vector transfected cells was subtracted from the uptake by Oatp1c1 transfected cells and data was normalized. Preliminary dose response curves as well as their corresponding tentative IC_{50} values were calculated using GraphPad Prism and listed in Table 1.

DISCUSSION

In the present study, immunohistochemical analysis of transiently transfected HEK293 cells displayed membrane localization of the Oatp1c1 protein. Oatp1c1 expression was also apparent within the ER in some of the stained cells which is consistent with previous studies [Westholm et al., 2009b]. Bidirectional transport of ^{3}H-E_2-17β-G was demonstrated in ER-derived vesicles and shown to be time dependent indicating Oatps may participate in the excretion of glucuronides from the ER lumen [Battaglia and Gollan, 2001]. Oatps/OATPs have multiple conserved N-glycosylation sites so post-translational modification is required within the ER and golgi apparatus. Lee et al., demonstrated mutagenesis of four predicted N-glycosylation sites on rat Oatp1a1 inhibited trafficking to the membrane and abolished substrate transport [Lee et al., 2003]. So, the appearance of Oatp1c1 expression in the ER membrane may be due to the post-translational processing of the Oatp sequence or due to its expression along the ER membrane.

PCR reactions using cDNA reverse transcribed from total mRNA isolated from transfected cells showed the Oatp1c1 gene was expressed in HEK293 cells after transfection. The sequence specific primers used were designed to give a PCR product spanning the Oatp1c1-V5/6xHis epitope tag junction to ensure the PCR product obtained was from the expression of the Oatp1c1-pEF-DEST 51 vector.

Uptake of ^{3}H-E_2-17β-G by Oatp1c1 transiently transfected cells showed a 4-fold increase over empty vector transfected cells and occurred in a time dependent manner. The uptake data was fit using an exponential equation model stating the rate of a

biological reaction is dependent upon concentration. The one phase association model is used to plot the interaction between a ligand and its receptor. However, when this equation was used to plot the curve-fit for the ^{3}H-E_2-17β-G uptake, the resulting R^2 value was 0.7680. The two-phase association model is used when the measured outcome, in this case the total uptake of ^{3}H-E_2-17β-G, is the result of a fast and a slow component. This resulted in an R^2 value of 0.8866. Based on this data, the uptake of ^{3}H-E_2-17β-G by Oatp1c1 appears to be the result of two binding sites and not one. Usually, uptake data is not fit with a curve. Due to the cost of reagents and previous data supporting the biphasic Oatp1c1-mediated uptake of ^{3}H-E_2-17β-G, the uptake data was curve fit to gain insight into Oatp1c1-mediated substrate binding [Westholm et al., 2009a].

Oatp1c1 has demonstrated multiple substrate binding sites as evidenced by the biphasic uptake curves of both T4 and E_2-17β-G [Westholm et al., 2009a]. Inhibition studies also demonstrated T4 and E_2-17β-G are competitive inhibitors of each other indicating they both share the same binding sites [Westholm et al., 2009a]. OATP2B1 has also demonstrated multiple binding sites as evidenced by the biphasic uptake of E-3-S, pravastatin and fexofenadine [Shirasaka et al., 2012 and 2014; Tamai et al., 2001]. And, both binding sites within OATP2B1 have demonstrated different pH sensitivities illustrating each substrate binding site within the active site my exhibit independence from the other [Shirasaka et al., 2012 and 2014; Tamai et al., 2001]. However, previous research completed by the Rumbley Laboratory, combined with the preliminary IC_{50} data presented here, make a case for Oatps/OATPs having one large active site accommodating multiple different substrates versus possession of two separate binding

sites.

Other enzymes involved with xenobiotic metabolism and display atypical kinetics are the CYPs. The active sites of CYPs are flexible allowing a vast range of possible substrates to bind and the ability of multiple substrates to bind simultaneously within the active site [Li and Poulos, 2004]. Specifically, CYP3A4 possess a single large flexible binding site able to accommodate multiple substrates at a time [Dabrowski et al., 2002; Ekroos and Sjögren, 2006; Kapelyukh et al., 2008; Torimoto et al., 2003]. The IC_{50} values calculated for each inhibitor was different depending on the CYP3A4 substrate they were tested against [Kapelyukh et al., 2008; Obach et al., 2006]. The different IC_{50} values could be explained by the number of substrate molecules able to bind at a single time in the active site versus the number of molecules the inhibitor is able to compete with, resulting in different reaction sensitivities for each substrate-inhibitor combination [Kapelyukh et al., 2008].

The preliminary IC_{50} data presented here, along with inhibition studies completed previously, is consistent with CYP3A4 data showing different concentrations of the same inhibitors are required to inhibit the Oatp1c1 uptake of T4 and E_2-17β-G [Westholm et al., 2009a]. For instance, pravastatin had an IC_{50} value of 197.3 μM against the uptake of T4 but a preliminary IC_{50} of 46.85μM against E_2-17β-G uptake (Table 1). This could indicate multiple molecules of pravastatin are binding in the active site of Oatp1c1 resulting in lowered affinity of E_2-17β-G binding, resulting in a decreased preliminary IC_{50} value for pravastatin. Also, the uptake ^{3}H-E_2-17β-G by OATP2B1 and Oatp1a4 was stimulated in the presence of low concentrations of estrone-3-glucuronide and

taurocholate, respectfully [Sugiyama et al., 2002; Tamai et al., 2001]. This data could indicate Oatps/OATPs are undergoing significant conformational changes when the first substrate molecule binds in the active site resulting in altered binding affinities for the second substrate molecule as is seen in CYP3A4 [Ekroos and Sjögren, 2006]. This data provides evidence for Oatps/OATPs possessing a single large active site able to simultaneously bind multiple substrate molecules. However, no conclusions regarding the active site of Oatp1c1 are drawn here due to the limited data set presented. Additional research is needed to address the structure and binding capacities of Oatp/OATP active sites.

In summary, Oatp1c1 was transcribed and translated after transfection within HEK293 cells. The Oatp1c1 protein was also found expressed within the cell membrane and the ER of transfected HEK293 cells. Uptake of ^{3}H-E_2-17β-G in Oatp1c1 transfected cells was 4-fold over empty vector transfected cells. Preliminary studies demonstrated all nine inhibitors tested inhibited the uptake of ^{3}H-E_2-17β-G to various degrees as evidenced by their different preliminary IC_{50} values. These preliminary IC_{50} values differed from those obtained during testing against the Oatp1c1-mediated uptake of T4. This data supports the notion of Oatp1c1 possessing one large binding site as opposed to multiple independent binding sites as seen in CYPs. However, further research is needed to determine the true nature of Oatp/OATP active site structure.

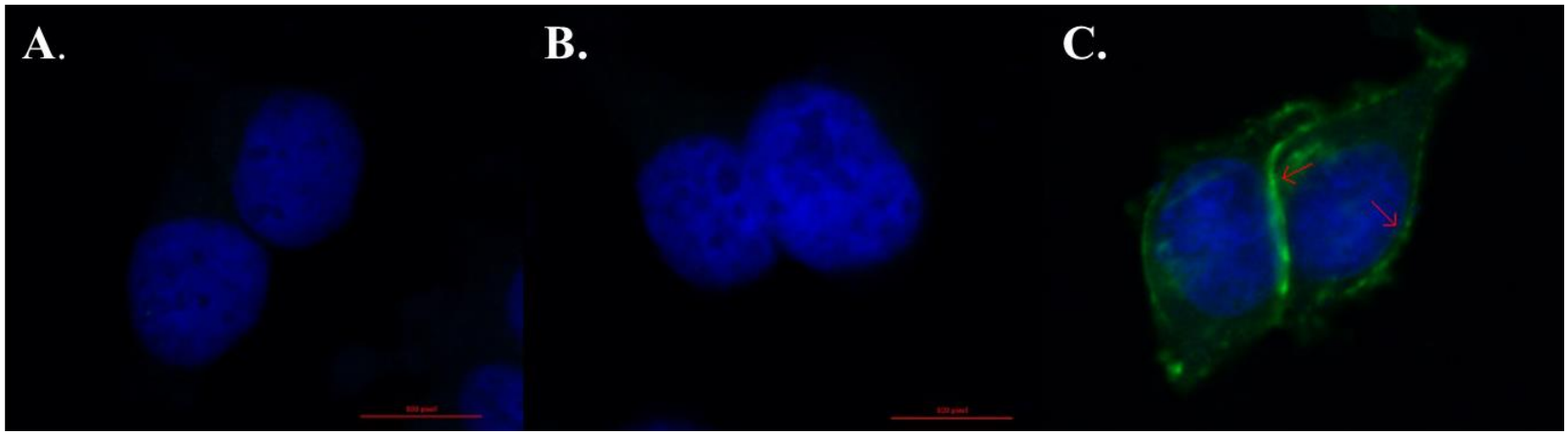

Figure 2. Immunohistochemistry of HEK293 Cells. Untransfected HEK293 cells (A), empty vector transfected (B) and Oatp1c1 transfected cells (C) were fixed to a 12mm poly-L-lysine coated glass coverslip and stained with an anti-V5-FITC antibody to reveal Oatp1c1 membrane localization (arrows). Blue stain corresponds to the nuclei of each cell and the green stain corresponds to Oatp1c1 localization.

A.

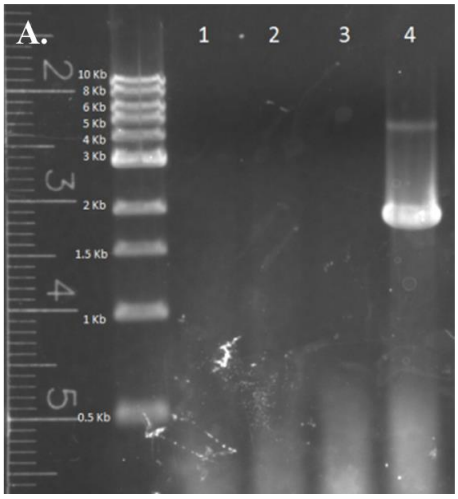

B.

Primer	Sequence 5'—3'
Oatp1c1 Forward	TCG-CAG-TTC-CCC-AGT-TCT-TC
V5/6xHis Forward	GTG-GTT-GAT-CTA-GGC-CC
V5/6xHis Reverse	TGA-TGG-TGA-TGA-TGA-CCG-GTA-CG

Lane No.	Cell Sample	Forward Primer	Reverse Primer
1	HEK293	V5/6xHis	V5/6xHis
2	HEK293	Oatp1c1	V5/6xHis
3	pEF-DEST 51	V5/6xHis	V5/6xHis
4	Oatp1c1	Oatp1c1	V5/6xHis

Figure 3. PCR Using Sequence Specific Primers. Total mRNA was isolated from untransfected, empty vector and Oatp1c1 transfected HEK293 cells and reverse transcribed into cDNA. Sequence specific primers were used to test for transcription and translation of Oatp1c1 from vector constructs. (A) PCR reactions using cDNA isolated from cells. (B) Table showing sequence specific primers and reactants for each lane in (A).

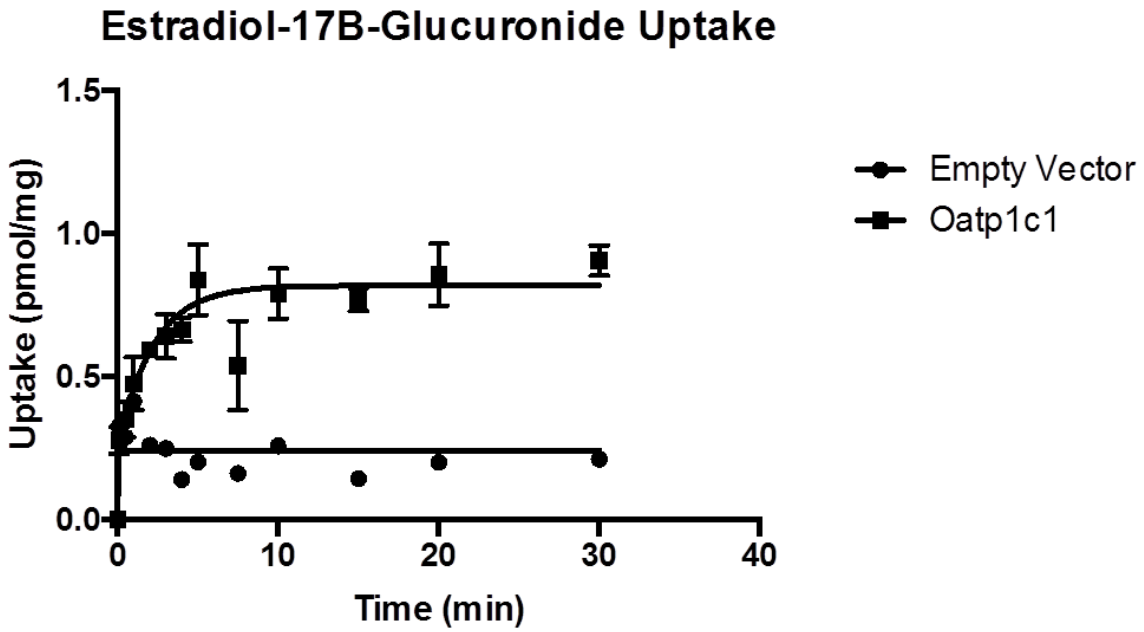

Figure 4. Estradiol Glucuronide Uptake. Empty vector transfected and Oatp1c1 transfected HEK293 cellular uptake of 55nM ^{3}H-E_2-17β-G was examined at various time points from 30sec to 30 min. Background radioactivity associated with a blank sample of 1% Triton X-100 was subtracted from all samples. Oatp1c1-mediated uptake of ^{3}H-E_2-17β-G was 4-fold greater than empty vector transfected HEK293 cells and happened in a time dependent manner. Uptake curve was fit using nonlinear regression (GraphPad Prism). Each point represents uptake mean± SE (n=3-6).

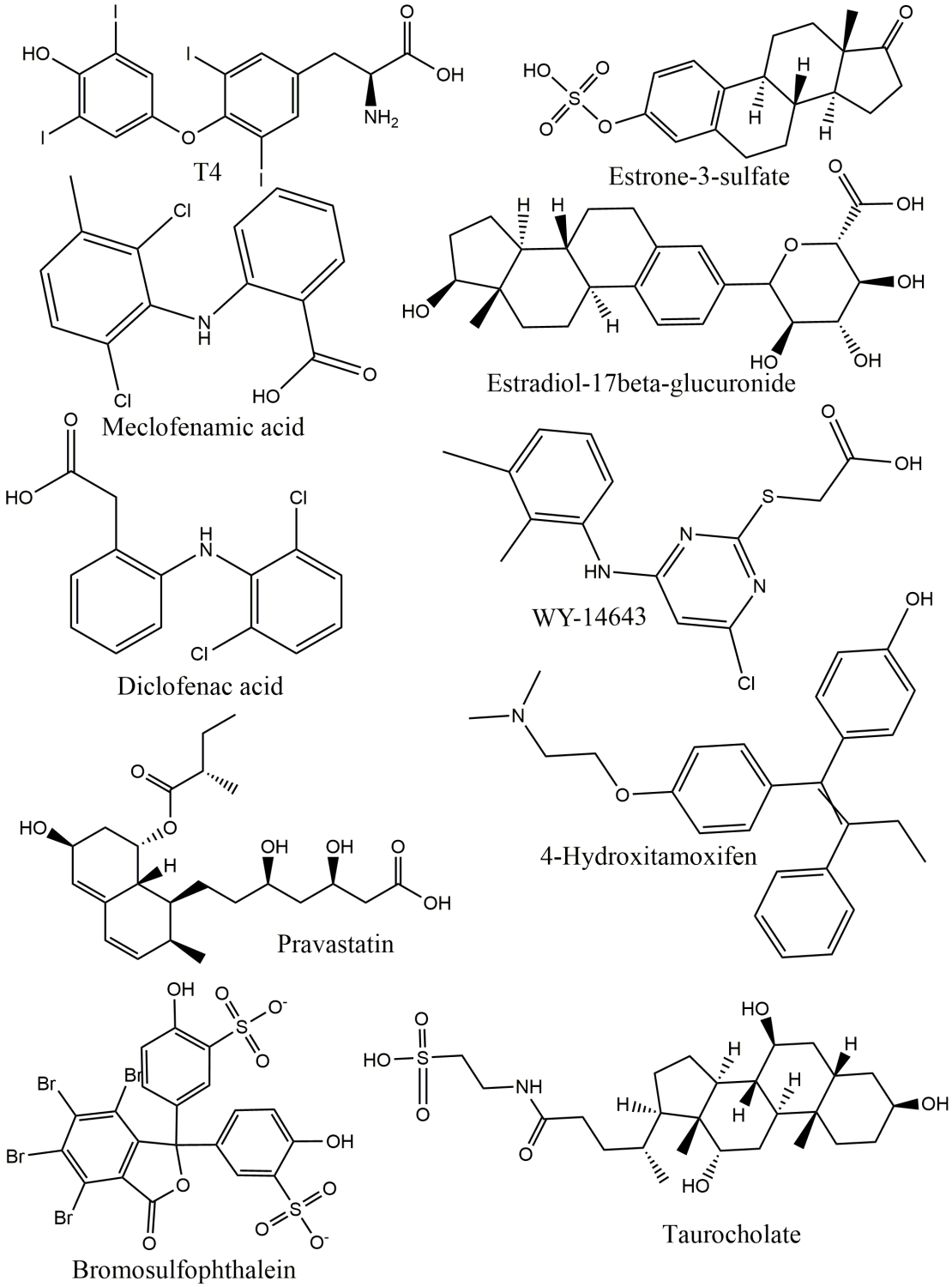

Figure 5. Chemical structure of Oatp1c1 substrate E_2-17β-G along with nine inhibitors tested. Structures were created using Chemdraw (PerkinElmer).

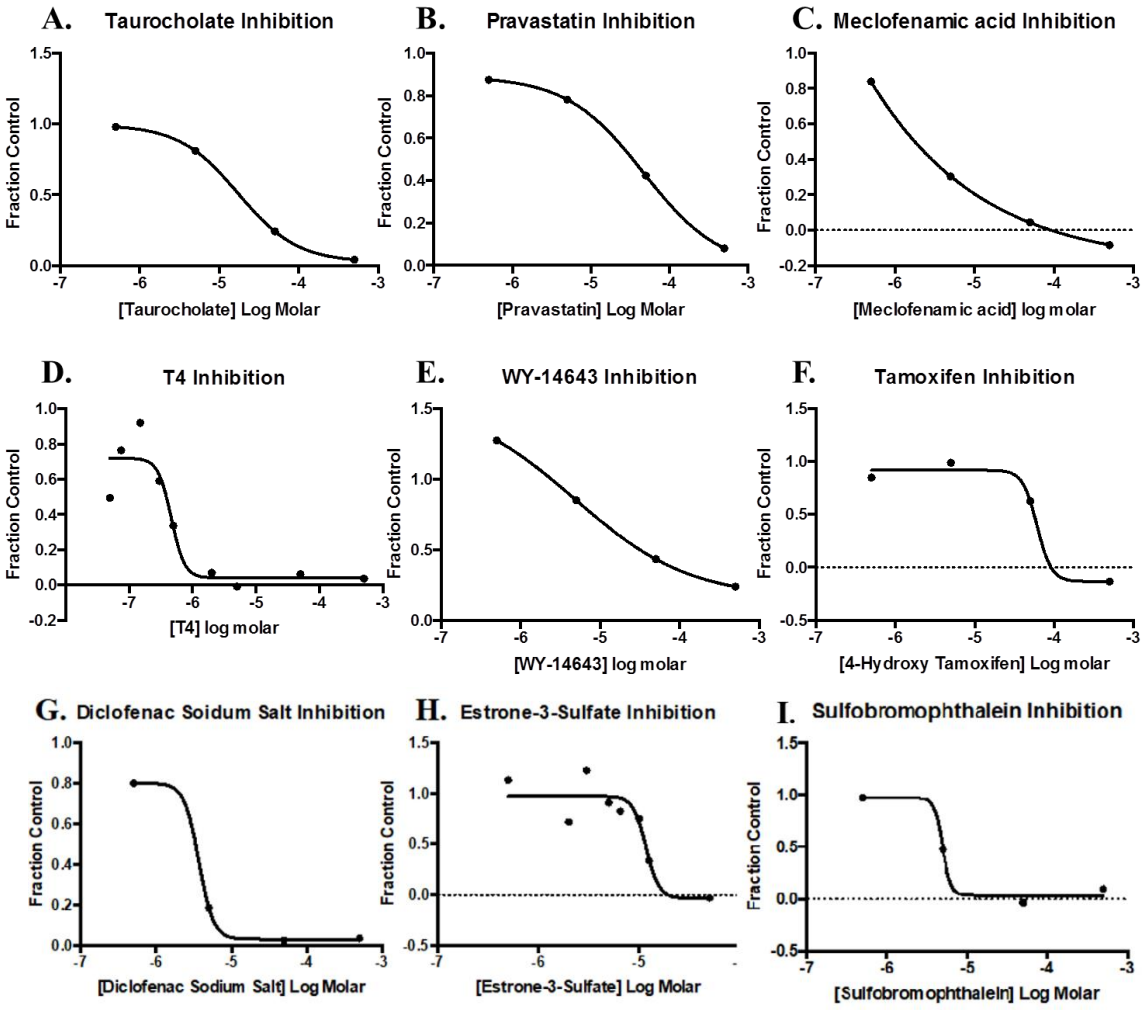

Figure 6. Oatp1c1 Dose Response Curves. Oatp1c1-mediated uptake of 55nM ^{3}H-E_2-17β-G in the presence of various inhibitor concentrations was measured after four minutes of incubation at 37°C. Dose response curves were fit using nonlinear regression (GraphPad Prism) and each point represents mean uptake ± SE (n=3-6).

Table 1. Preliminary IC_{50} values for Oatp1c1 Transport Inhibitors

Estradiol Glucuronide Inhibition		Thyroxine Inhibition	
Inhibitor	**Prelim. IC_{50} (uM)**	**Inhibitor**	**IC_{50} (uM)**
BSP	4.93	BSP	0.81
Estrone-3-sulfate	6.12	Estrone-3-sulfate	2.47
Meclofenamic acid	2.68E-05	Meclofenamic acid	3
Diclofenac acid	3.676	Diclofenac acid	4
WY-14643	4.744	WY-14643	15.1
Taurocholate	17.3	Taurocholate	29.05
4-hydroxytamoxifen	61	4-hydroxytamoxifen	33.1
T4	46.38	Estadiol glucuronide	81
Pravastatin	46.85	Pravastatin	197.3

IC_{50} values for each substrate were calculated using nonlinear regression (GraphPad). Values for Estradiol Glucuronide inhibition were calculated from a single dose response curve and hence labeled as preliminary values.

Chapter 2

Phylogenetic analysis of the Organic Anion Transporting Polypeptide Family

SYNOPSIS

Organic anion transporting polypeptides (Humans: OATPs, all others: Oatps), are promiscuous membrane transporters that recognize and transport numerous unrelated amphipathic anions including hormones and their conjugates, bile salts, and various endobiotics and xenobiotics. Interestingly, these sodium-independent, bidirectional solute transporters are highly conserved proteins present in all metazoans sequenced to date but are absent in all other organisms including bacteria, fungus and plants. Sequence alignments of *Homo sapiens* OATPs with that of primitive organisms have shown Oatp/OATP proteins have a high level of evolutionary conservation. The promiscuity displayed by Oatps/OATPs has made understanding Oatps/OATPs overall physiological role difficult. Understanding why such primitive organisms like *Monosiga, Trichoplax* and *Nematostella* possess Oatps may allow for the clarification of the evolved physiological role of Oatps/OATPs. Due to the high level of conservation of Oatps/OATPs among all metazoans, understanding what physiological purpose these transport proteins are serving is important, especially since Oatps/OATPs are present in such a diverse range of environments and nutrient availability.

For comprehensive phylogenetic analysis of the Oatp family, *H. sapiens* OATP4A1 protein sequence was used as the query sequence for BLASTp searches completed against organisms with complete or nearly complete genomes. Multiple sequence alignments of all 1264 protein sequences were completed using MAFFT, QuickProbs and Clustal Omega. These alignments were compared to one another and subsequently submitted to FastTree 2.0 and MrBayes 3.2 for phylogenetic tree construction and

analysis. *Amphimedon queenslandica* was revealed to be the first true metazoan to possess Oatp sequences and these sequences are more Oatp4-like than any other Oatp family, likely indicating the Oatp4 family was the first to evolve. A seventh Oatp cluster was discovered and labeled here as the Uncharacterized Oatp cluster. Protein sequences belonging to the Uncharacterized Oatp cluster appear in metazoan evolution after the Bilaterian clade split into Protostomia and Deuterostomia, and linger until the evolution of vertebrates where sequences in the Uncharacterized Oatp cluster become lost.

INTRODUCTION

Oatps/OATPs are promiscuous bidirectional membrane transporters able to transport numerous unrelated amphipathic anions including hormones and their conjugates, bile salts and various endobiotics and xenobiotics. Oatps/OATPs have varying tissue expression profiles with some Oatps/OATPs having discrete tissue-specific expression and some Oatps/OATPs having ubiquitous expression. Oatps/OATPs are grouped into families (≥40% amino acid sequence identity) and subfamilies (≥60% amino acid sequence identity) with human OATPs forming six families (OATP1-OATP6) and ten subfamilies (OATP1A-OATP6A) [Hagenbuch and Meier, 2003].

Oatps belong to the solute carrier (SLC) family of membrane transporters and the SLC family is the second largest family of membrane proteins. A large number of SLC families found in humans are highly evolutionarily conserved among bilaterians [Höglund et al., 2011]. A majority of SLC families found in *Homo sapiens* are also found in *Caenorhabditis elegans* and *Nematostella vectensis* [Höglund et al., 2011]. The SLC family is present throughout the entire Eukaryota lineage whereas the Oatp family is restricted to animals [Höglund et al., 2011]. Oatps are found in all metazoans sequenced to date including some of the most primitive metazoans *N. vectensis* and *Trichoplax adhaerens*, as well as in the choanoflagellate *Monosiga brevicollis*.

The presumably most primitive Oatp is present in the choanoflagellate, *M. brevicollis*. Choanoflagellates are the closest unicellular relatives to the metazoans. Choanoflagellates are single-celled organisms with a single apical flagellum surrounded by a ring of microvilli. *T. adhaerens* is an aquatic placozoan and has the simplest body

organization of all living metazoans consisting of only four different cell types. *T. adhaerens* has no internal organs, no specialized muscle or nerve cells and has no symmetry or polarity. *N. vectensis* is an aquatic cnidarian and has a sac-like body plan with a single oral opening surrounded by tentacles. *N. vectensis* is the most primitive animal with organized tissues including specialized cells from muscle, neuronal and epithelial tissues [Putnam et al., 2007]. All three of these organisms live in an aquatic environment and have simple body plans yet possess membrane transporters such as Oatps.

To help elucidate why such simple organisms would possess membrane transporter proteins such as Oatps, an effort was made to reconstruct the evolutionary history of the Oatp family. The process of understanding the evolution of a protein family through phylogenetic analysis is not a novel approach. However, this approach has never been performed on the Oatp family. Many functional and substrate transport characterization studies have been completed on various members of the Oatp/OATP family but none have ever looked into the evolutionary development of the Oatp/OATP family. Due to their high level of conservation throughout metazoan evolution, insight into the evolved physiological role of Oatps/OATPs can be gained from a comprehensive phylogenetic analysis.

Multiple Sequence Alignments

In the present study, homologous Oatp sequences were collected and aligned using three different multiple sequence alignment programs: Clustal Omega, MAFFT and QuickProbs. Multiple different alignment programs where chosen because each program

uses a different method for aligning protein sequences. Clustal Omega uses mBed consisting of embedding each sequence in space and replacing it with a vector [Sievers et al., 2011; Söding, 2005]. The distance between these vectors in space represents the dissimilarity between the sequences and the vectors are then clustered via unweighted pair group method with arithmetic mean (UPGMA) and aligned very quickly using hidden Markov models [Sievers et al., 2011; Söding, 2005]. MAFFT, using the G-INS-1 algorithm, creates an alignment by first building a progressive guide tree through fast Fourier transform and dynamic programing. This ensures two sequences are optimally aligned before additional sequences are added to the guide tree. This involves much more rigorous calculations than other alignment programs [Katoh et al., 2002; Long et al., 2016; Yamanda et al., 2016]. QuickProbs follows the same 4-step alignment process as MSAProbs which combines pair hidden Markov models and partition functions in order to calculate the posterior probability for all sequence pairs [Gudyś and Deorowicz, 2014; Liu et al., 2010]. After this, QuickProbs employs two other methods, consistency transformation and profile-profile alignments, to remove error or inaccuracy introduced into the alignment [Gudyś and Deorowicz, 2014; Liu et al., 2010]. QuickProbs is also specifically customized for graphics processors proving to be more accurate and 5-9x's faster than other alignment programs [Gudyś and Deorowicz, 2014].

Phylogenetic Tree Construction

To build phylogenetic trees using all three multiple sequence alignments, character-based methods of phylogenetic analysis were chosen over distance-based methods for their approach of comparing one amino acid at a time over the entire protein sequence

[Yang and Rannala, 2012]. Of the character-based methods, maximum likelihood and Bayesian analysis were chosen because of their ability to use complex and biologically relevant amino acid substitution models [Yang and Rannala, 2012]. Before the alignments were submitted for phylogenetic analysis, PhyML Smart Model Selection was used to determine the best fit amino acid substitution model for this data set, resulting in Whelan and Goldman (WAG) with gamma distribution [Whelan and Goldman, 2001]. WAG differs from other amino acid substitutions models by incorporating the possibility of multiple amino acid substitutions taking place along any given branch as opposed to only one amino acid substitution.

Both maximum likelihood and Bayesian methods rely on the likelihood function, but the way each method handles their parameters is quite different [Huelsenbeck and Ronquist, 2002]. FastTree 2.0 and MrBayes 3.2 where chosen to construct phylogenetic trees by maximum likelihood and Bayesian analysis methods, respectfully. Maximum likelihood works to determine the phylogenetic tree topology that confers the highest likelihood with a given set of data and specific amino acid substitution model [Yang and Rannala, 2012]. FastTree 2.0 software infers maximum likelihood trees by first constructing a tree using neighbor joining and minimum evolution methods and further improving the tree with subtree-pruning-regrafting [Price et al., 2010]. Bayesian inference relies on the posterior probability, or the probability the given phylogenetic tree is evolutionarily correct [Page, 2003; Yang and Rannala, 2012]. Before data analysis, parameters within the chosen model are assigned statistical distribution and then combined with the data set to calculate posterior probabilities [Huelsenbeck et al., 2002,

Yang and Rannala, 2012]. MrBayes 3.2 software was utilized for Bayesian inference methodologies allowing for the convergence of posterior probabilities to be monitored and the use of multiple processor threads in parallel [Ronquist et al., 2012].

In the present study, complete and nearly complete genomes where searched for Oatp homologs using the Basic Local Alignment Search Tool (BLASTp) on the National Center for Biotechnology (NCBI) website using *Homo sapiens* OATP4A1 protein sequences as the query sequence. The OATP4A1 sequence was used because the Oatp4 family is thought of as the oldest or most conserved of all Oatp families. Homologous Oatp sequences were found in a diverse range of taxa spanning the evolutionary distance between sponges and humans. In total, 1264 protein sequences were collected and submitted to three different alignment programs for multiple sequence alignment. In this case, Clustal Omega, MAFFT and QuickProbs alignment programs were used to align all protein sequences. For comprehensive phylogenetic analysis, maximum likelihood and Bayesian inference methodologies where chosen as best fit for this data collection and FastTree 2.0 and MrBayes 3.2 software were utilized to build phylogenetic trees. This resulted in a total of six phylogenetic trees. All three trees constructed using FastTree 2.0 resulted in an overall similar topology with seven Oatp clusters. The seventh, labeled here as the Uncharacterized Oatp cluster, is reported first here. However, the three trees constructed using MrBayes 3.2 did not reach consensus, leaving a majority of branches originating from a single node in the center of the tree.

MATERIALS AND METHODS

Sequence Collection and Alignments

Multiple searches for Oatp/OATP protein sequences were performed using NCBI (https://blast.ncbi.nlm.nih.gov/Blast.cgi) BLASTp tool [Altschul et al., 1990]. *Homo sapiens* OATP4A1 amino acid sequence (NP_057438.3) was used as the query sequence while performing BLASTp searches against organisms with complete or nearly complete genomes with an E-value cutoff of 10^{-6}. Once all sequences were collected, Clustal X 2.1 [Larkin et al., 2007] was utilized to build smaller alignments of species within the same phylum to aid in the elimination of partial and duplicate sequences (using default settings). Multiple sequence alignments of all remaining protein sequences, totaling 1264, were then made using MAFFT v7.029 (http://mafft.cbrc.jp/alignment/server/large.html?17jul) utilizing G-INS-1 algorithm with an open gap penalty of 2.1 and an extend penalty of 0.72 [Katoh et al., 2002; Long et al., 2016; Yamanda et al., 2016], QuickProbs using default settings [Gudyś and Deorowicz, 2014], and Clustal Omega (http://www.ebi.ac.uk/Tools/msa/clustalo/) utilizing the default algorithm [Sievers et al., 2011]. The multiple sequence alignments were compared with one another and used for further phylogenetic analysis.

Phylogenetic Analysis

Before phylogenetic analysis, an alignment file containing all 1264 protein sequences was submitted to PhyML [Lefort et al., 2017] for Smart Model Selection. The resulting amino acid substitution model, WAG using gamma distribution, was used for phylogenetic analysis by both maximum likelihood and Bayesian inference methods

[Whelan and Goldman, 2001]. FastTree software was utilized on multiple processor cores for maximum likelihood phylogenetic analysis with the following input command: fasstreeMP -wag -gamma filein > fileout [Price et al., 2010]. MrBayes was utilized on four processor cores for Bayesian inference by first using Mesquite [Maddison and Maddison, 2017] to open data files and reformat for export into MrBayes. The following input commands batch file was used for MrBayes: set autoclose=yes nowarn=yes; lset rates=gamma; prset aamodelpr=fixed(wag); mcmcp ngen= 400000 relburnin=yes burninfrac=0.25 printfreq=2000 samplefreq=2000 nruns=2 nchains=2 savebrlens=yes; mcmcp Checkfreq=50000; mcmc; sumt; end [Ronquist and Huelsenbeck, 2003]. The resulting phylogenetic trees were visualized using The Interactive Tree of Life (http://itol.embl.de/) and Dendroscope v3.5.9 [Huson and Scornavacca, 2012].

Computer Description

MrBayes, FastTree and QuickProbs were all run locally on an Exxact Grp. Quantum TXR410-512R workstation with 2 Xenon E2-2620 processors, 32 Gb ram and 2 Geforce GTX 770 GPUs.

RESULTS

Identifying Oatp Homologs

In the present study, comprehensive phylogenetic analysis of homologous Oatp sequences was completed on species with complete or nearly complete sequenced genomes. *H. sapiens* OATP4A1 protein sequence, 722 amino acids in length, was used as the query sequence for BLASTp searches on the NCBI website resulting in sequence collection from over 250 organisms. Using Clustal X, partial, duplicate and trivial isoform variant sequences were eliminated from the analysis leaving 1264 total protein sequences. No homologous Oatp sequences were detected in the genomes of bacteria, fungus or plants despite extensive searches.

Multiple Sequence Alignments

To investigate the evolutionary relationship between Oatp homologs, comprehensive phylogenetic analysis was conducted over the span of each entire protein sequence. A fasta formatted file containing all 1264 protein sequences was submitted to the online multiple sequence alignment programs Clustal Omega, MAFFT and QuickProbs. Each of these three programs gave varying alignment results likely due to the differences in algorithms and gap settings. Fig.1 illustrates some of the similarities and differences seen between the three multiple sequence alignments. The same stretch of amino acids within each of the three alignments is depicted (Fig. 1A-C) showing the columns and gaps are quite similar and exhibit minimal spacing, indicating a lack of sequence divergence in this stretch of amino acids. The highly conserved 13-amino acid Oatp/OATP superfamily signature D-X-RW-(I,V)-GAWW-X-G-(F,L)-L is part of the

protein sequence shown (Fig.1A-C) so consensus among the alignments is not surprising. Fig. 1D-F also depicts a similar stretch of amino acids within all three alignments but illustrates an area where differences arise. This is evidenced by the tight clustering of columns in Fig. 1D whereas Fig. 1E-F has large gaps and sporadically placed columns of amino acids. Also, notice the lack of overall gaps in Fig. 1A and Fig. 1D, the Clustal Omega alignment, as Clustal Omega has a larger default gap open penalty (6 bits) than any of the other alignment servers used.

Phylogenetic Trees

Each of the three multiple sequence alignments were submitted to both FastTree 2.0 and MrBayes 3.2 for phylogenetic tree construction. FastTree 2.0 gave very similar results for all three trees constructed whereas MrBayes 3.2 did not fully converge, leaving all three trees compact with minimal branching. MrBayes 3.2 was set to run for 400,000 generations but additional generations were needed for full convergence on a consensus tree. Due to time constraints, new trees were not generated.

Fig. 2 illustrates each of the phylogenetic trees as radial phylograms with all 11 of the *H. sapiens* OATP proteins highlighted. Each of the phylogenetic trees constructed using FastTree 2.0 resulted in similar overall topologies (Fig. 2A, C, and E). This includes the nodes for the Oatp4, Oatp5 and Oatp6 clusters branching close on one side of the tree with the nodes of the Oatp1, Oatp2 and Oatp3 clusters branching close on the other side of the tree and the node for the Uncharacterized Oatp cluster in-between. No conclusions are drawn from the MrBayes 3.2 trees since each failed to reach consensus as evidenced by the origination of most branches from a single node in the center of the

phylogram (Fig. 2B, D and F).

The similar overall topologies of the FastTree 2.0 phylogenetic trees is more clearly illustrated in Fig. 3 where all of the Oatp clusters are labeled, including the 11 *Homo sapiens* OATP proteins. Notice there are no *H. sapiens* OATPs branching in the Uncharacterized Oatp cluster. The Uncharacterized Oatp cluster is made up of mainly species of the phylum Arthropoda and Nematoda.

Phylum Nematoda

Oatps/OATPs are grouped into families and subfamilies based on amino acid sequence identity with >40% amino acid sequence identity denoting families and >60% denoting subfamilies [Hagenbuch and Meier, 2003]. Analysis of species within the phylum Nematoda included in this study revealed nematodes have Oatp proteins branching within only two Oatp clusters, the Oatp4 and the Uncharacterized Oatp cluster (Fig. 4A). The Oatp proteins appearing in the Oatp4 cluster form three separate families based on the criteria mentioned above excluding sequences within *Trichinella*. The two *Trichinella* species included in this analysis each have one sequence appearing to branch within the Oatp4 cluster and these *Trichinella* sequences seem to form their own family because they are only 30-37% identical to the sequences within the three families (data not shown). All four of these families are considered Oatp4-like families because the branch nodes are close to the nodes of the Oatp4 cluster (Fig. 4B).

The Oatp proteins appearing within the Uncharacterized Oatp cluster also form three separate families with *Trichinella* species again forming a fourth family of their own (data not shown). In this case, the *Trichinella* sequences have a higher percent

identity (32%-38% identical) to sequences within these three families (data not shown). Because this *Trichinella* specific family just misses the 40% identity cutoff with one of the Uncharacterized Oatp-like families, these two families were combined into one to form a total of three families within the Uncharacterized Oatp cluster. The nodes for these three families branch within the Uncharacterized Oatp cluster so they are considered Uncharacterized Oatp-like families.

Phylum Arthropoda

Analysis of all species within the phylum Arthropoda included in this study revealed arthropods possess Oatp proteins branching within three different Oatp clusters (Fig. 5A). Almost all of the arthropod species analyzed have an Oatp protein branching within both the Oatp4 cluster and the Oatp5 cluster (Fig. 5B). The nodes for protein sequences branching in both of these clusters are close to the nodes for the Oatp4 and the Oatp5 families so they are labeled as Oatp4-like and Oatp5-like families, respectfully. The protein sequences within the Oatp4-like family form two separate subfamilies, one consisting of only two sequences. However, these two sequences range from 53%-57% identical to the rest of the sequences within the Oatp4-like family, so all of the sequences within the Oatp4-like family were considered part of the same subfamily. Protein sequences within the Oatp5-like family are all greater than 60% identical and were also grouped into one subfamily.

All of the other Oatp protein sequences possessed by Arthropods branch within the Uncharacterized Oatp cluster (Fig. 5B). Sequence identity calculations revealed the sequences branching within the Uncharacterized Oatp cluster form four families (data not

shown). Because the nodes for all four of these Oatp families branch within the Uncharacterized Oatp cluster they are all considered to be Uncharacterized Oatp-like. One of these Uncharacterized Oatp-like families is specific to species of the class Insecta and order Diptera. The largest Uncharacterized Oatp-like family was originally broken into three different families due percent identities <40%. However, these three families where later combined into a single large family due to a majority of the percent identities being 35%-38%.

Class Aves

All of the modern bird species included in this study, of phylum Chordata and class Aves, collectively have Oatp proteins branching within all Oatp clusters except for the Uncharacterized Oatp cluster (Fig. 6A). Also of interest, of the 31 species included in this analysis, only two bird species do not possess an Oatp1c1 and only seven bird species have an Oatp of the Oatp1b subfamily (Fig. 6B). Oatp1c1 is expressed within the choroid plexus and the hypothalamus of Japanese Quail and has shown a high affinity for thyroid hormones indicating a role in the photoperiodic response of the gonads [Nakao et al., 2006]. Of interest is the lack of species with Oatp proteins of the Oatp1b subfamily as they are discreetly expressed within the sinusoidal membrane of the liver within rodents and humans where these proteins work to uptake and eliminate a wide range of endo- and xenobiotics [Hagenbuch and Meier, 2003]. This could be due to sequencing errors or gaps as this data is completely reliant on divergent sequence qualities and computational protein generation. However, there could be an evolutionary reason behind the lack of Oatp1b's due to the diets of Aves.

Early Evolution of Oatps

T. adhaerens and *N. vectensis* are primitive metazoans and are considered among the first organisms to possess Oatp proteins. In the case of this study, *N. vectensis* was used as the starting point to track the change in the evolutionary time line where species evolved from possessing multiple closely related, presumable functionally similar Oatp sequences to having more divergent Oatp sequences with presumably unique functions (Fig. 7). The model organism *N. vectensis* was chosen because Cnidarians are the most primitive metazoans with organized tissues and specialized cell types and *N. vectensis* possesses twelve similar yet separate Oatp proteins. Beginning with *N. vectensis*, nodes where counted to reveal *Amphimedon queenslandica*, *Acropora digitifera* and *Hydra vulgaris* as the closest branching species to *N. vectensis* with *A. queenslandica* and *A. digitifera* both having two Oatp proteins (Fig. 7). *A. queenslandica* and *A. digitifera* both possess only two Oatp proteins more closely identical to the Oatp4 family than to any other Oatp family. Further along the evolutionary time line, the branch nodes for Sea Urchin (*Strongylocentrotus purpuratus*), *Saccoglossus kowalevskii*, and *Ciona intestinalis* appear, and each of these three organisms have seven to eight Oatp proteins (Fig. 7B). So, the evolutionary distance from *N. vectensis* to *C. intestinalis* represents the transition from having multiple sequentially similar Oatp proteins to having fewer more divergent Oatp proteins, and eventually having multiple Oatps.

DISCUSSION

Many research studies have focused on the transport properties of Oatps/OATPs but few have done any phylogenetic analysis of the Oatp family. Here, a comprehensive phylogenetic analysis was completed on the entire Oatp family enabled by the growing number of protein sequences and sequenced genomes available. Homologous Oatp/OATP sequences were found in a diverse range of taxa, spanning the evolutionary distance from sponges to humans. In search of homologous sequences, numerous BLASTp searches were conducted against species with complete or nearly complete genomes using *H. sapiens* OATP4A1 protein sequence as the query sequence. Each BLASTp search resulted in multiple sequences for each Oatp/OATP protein and only the isoform with the longest sequence and highest percent identity to the query sequence was selected for analysis. Of the sequences saved for analysis, clearly partial or duplicates of other sequences were eliminated to decrease the error introduced into the analysis. Also, this analysis is based on the protein sequences listed on NCBI as of January 2017. Since then, amendments to already existing sequences were made as well as additional sequences added, making this analysis already incomplete.

Each multiple sequence alignment program has a different method for aligning protein sequences so multiple programs were used to align all 1264 protein sequences. This resulted in dissimilar alignments with varying levels of accuracy. Clustal Omega had the highest gap open penalty setting of 6 bits, causing the Clustal Omega multiple sequence alignment to have minimal gaps between amino acids whereas MAFFT had a gap open penalty of 2.1 bits resulting in additional gaps over Clustal Omega. For this

reason, the Clustal Omega multiple sequence alignment was used as the resulting phylogenetic tree was easier to read.

Of the two phylogenetic tree construction programs used, FastTree 2.0 gave similar resulting trees whereas MrBayes did not fully converge on a consensus tree for any of the three alignments leaving the trees unbranched. A rough estimate of the calculation time needed for MrBayes to reach a consensus tree was 10+ days leaving the phylogenetic observations completed here performed on the maximum likelihood trees.

What is believed to be the first Oatp is found in the choanoflagellate *M. brevicollis*. After comprehensive phylogenetic analysis of the Oatp family, *A. queenslandica* was discovered as the first metazoan to possess Oatp proteins based on *A. queenslandica* Oatp sequences aligning with the Oatp sequence from *M. brevicollis* and the position of *A. queenslandica* within the first branching phylum of metazoan evolution. The next species to possess Oatp proteins are *T. adhaerens*, *N. vectensis*, *A. digitifera* and *H. vulgaris*. All of these organisms are primitive metazoans, emerging before the bilaterian clade. *A. queenslandica* and *A. digitifera* only have two Oatp proteins, both most alike the Oatp4 family. The Oatp sequences of *A. queenslandica* have a 28%-31% amino acid identity with *H. sapiens* OATP4A1 sequence and the Oatp sequences of *A. digitifera* are both 35% identical to *H. sapiens* OATP4A1 sequence. *T. adhaerens* and *N. vectensis* both have multiple Oatp proteins more similar to each other than to any other Oatp but are most alike the Oatp4 family. Also, the recent sequencing of the *T. adhaerens* genome revealed a gene closely related to the sequence of *H. sapiens* OATP4C1 underwent multiple tandem duplication events leading to over twenty copies of this gene [Srivastava

et al., 2008]. This data combined indicates *A. queenslandica* was the first metazoan to possess Oatp proteins and the Oatp4 family was likely the first family to evolve. Oatp proteins also underwent a species-specific expansion within both *T. adhaerens* and *N. vectensis*.

Once Bilateria splits into the clades Protostomia and Deuterostomia, a new family of Oatp proteins emerge labeled as the Uncharacterized Oatp cluster in Fig. 3. Of the phyla representing Protostomia, Nematoda and Arthropoda were more closely analyzed. What was previously thought of as only two families of Oatp proteins within nematodes was actually identified as seven families using percent identity calculations. Four different families branch within the Oatp4 cluster, one *Trichinella* specific, and three families branch within the Uncharacterized Oatp cluster again with one family *Trichinella* specific. Each of these families are considered Oatp4-like or Uncharacterized Oatp-like as their nodes are still within, or close to, the nodes of their respective families. This evidence suggests gene duplication took place within *Trichinella* species because they form an Oatp family of their own within the Oatp4 and the Uncharacterized Oatp clusters.

Arthropods, on the other hand, were found to have six families of Oatp proteins. Two of these six families fall within the already recognized Oatp families, the Oatp4 and the Oatp5, and hence were considered Oatp4-like and Oatp5-like, respectfully. The other four families are part of the Uncharacterized Oatp cluster. Not only did this new Oatp cluster, the Uncharacterized Oatp cluster, emerge with the evolutionary split of Protostomia and Deuterostomia, but it appears this new Oatp cluster expanded within the

arthropods as evidenced by the larger number of Oatp proteins within the Uncharacterized Oatp cluster over those present in nematodes.

Deuterostomia is made up of three clades, Echinodermata, Hemichordata and Chordata. Species within all three of these clades, *S. purpuratus, S. kowalevskii* and *C. intestinalis,* still have Oatp proteins branching within the Uncharacterized Oatp cluster as seen in Fig. 7A. However, the Uncharacterized Oatp cluster seems to get lost somewhere along the chordate lineage before the divergence of vertebrates. The chordate lineage is marked by large-scale DNA duplications creating many of the gene families seen in vertebrates [McLysaght, Hokamp and Wolfe, 2002]. There is also evidence of gene families from ancestral chordates becoming independently diversified among the chordate and vertebrate lineages [Dehal et al., 2002]. This independent diversification of gene families through the chordate and vertebrate lineages combined with the large-scale DNA duplications within the early chordate lineages could explain the difference we see between the seven Oatp proteins within the genome of *C. intestinalis,* including the presence of Oatp proteins within the Uncharacterized Oatp cluster, and the twelve divergent Oatp proteins we see in the vertebrate *H. sapiens,* with the noticeable absence of the Uncharacterized Oatp cluster.

In summary, comprehensive phylogenetic analysis of the Oatp family has shown *A. queensladica* is the first metazoan to possess Oatp proteins and the Oatp4 family was likely the first to evolve. Oatps group into seven clusters with data presented here the first to show the presence of the seventh Oatp cluster, the Uncharacterized Oatp cluster. Proteins within the Uncharacterized Oatp cluster did not evolve until the Bilaterian split

of Protostomia and Deuterostomia and proteins within this cluster linger until the evolution of vertebrates where these proteins become lost. The mechanism of Oatp evolution is likely a mixture of mutations, genetic drift and gene duplications in early metazoan evolution. Large-scale DNA duplications in early chordate lineage as well as the independent diversification of the Oatp family within vertebrates is also likely to play a role. There is also evidence of species-specific expansion of the Oatp families presented here for *T. adhaerens* and *Trichinella* species as well as many species within the phylum Arthropoda. The physiological role Oatps/OATPs evolved for is still unclear. With further research into the genomes of primitive metazoans, this will aid in understanding of the evolved physiological role of Oatps/OATPs.

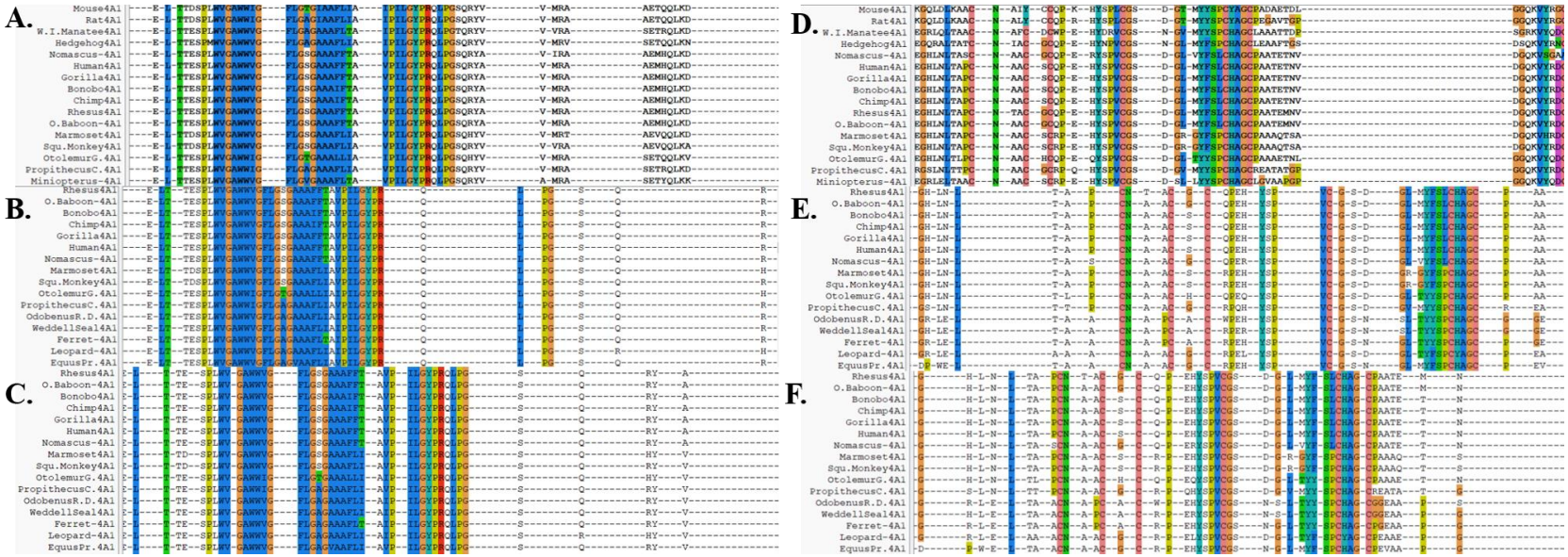

Figure 1: Alignment Patterns Seen in Multiple Sequence Alignments. Snap shot from each of the 3 alignment programs used. (A) and (D) Clustal Omega, (B) and (E) MAFFT, (C) and (F) QuickProbs. The same stretch of amino acids from all three alignments are shown to illustrate an area of similarity in A-C and an area of dissimilarity in D-F. The portion of the sequence depicted in A-C contains the 13-amino acid Oatp superfamily signature.

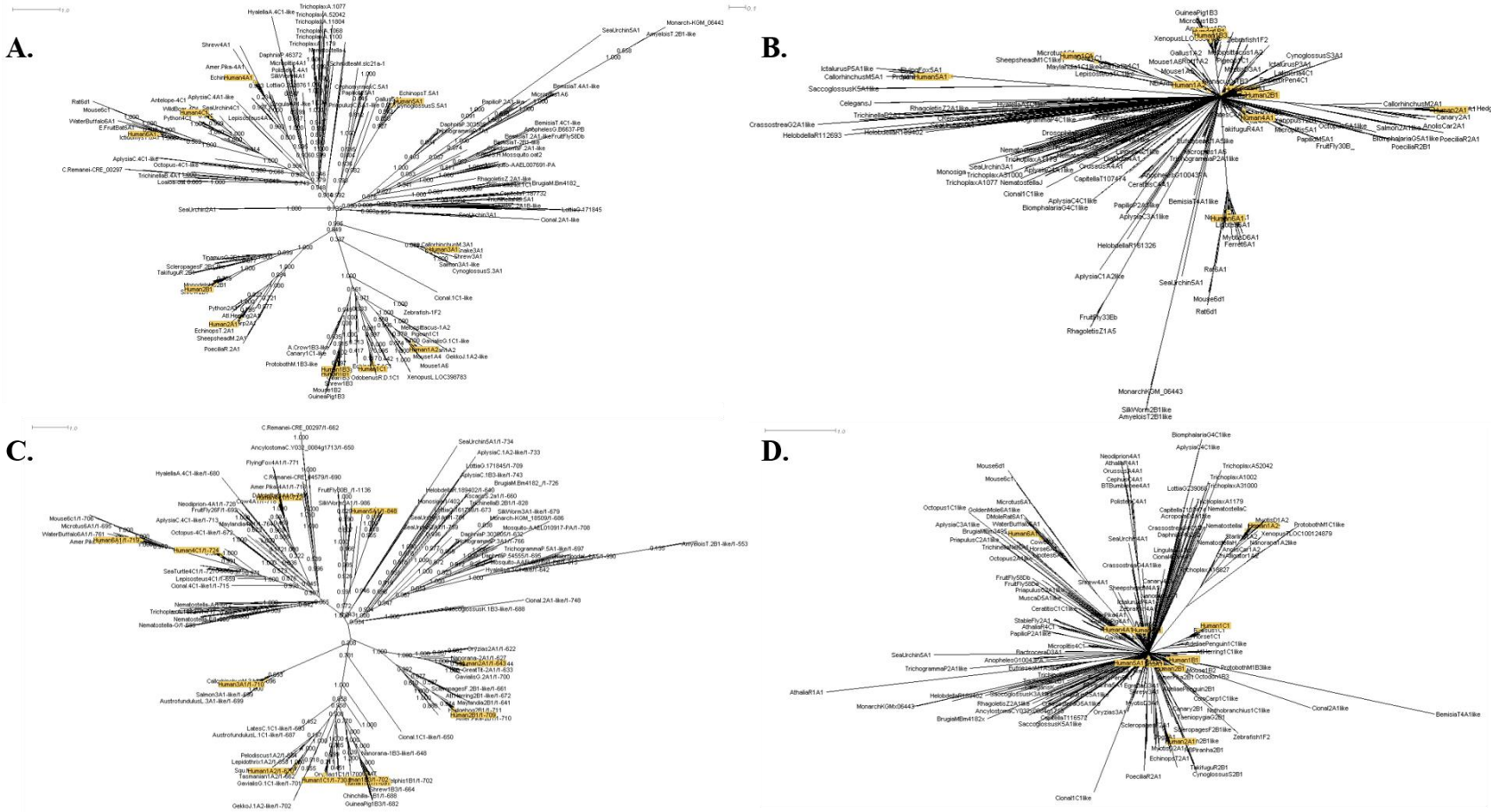
A.
B.
C.
D.

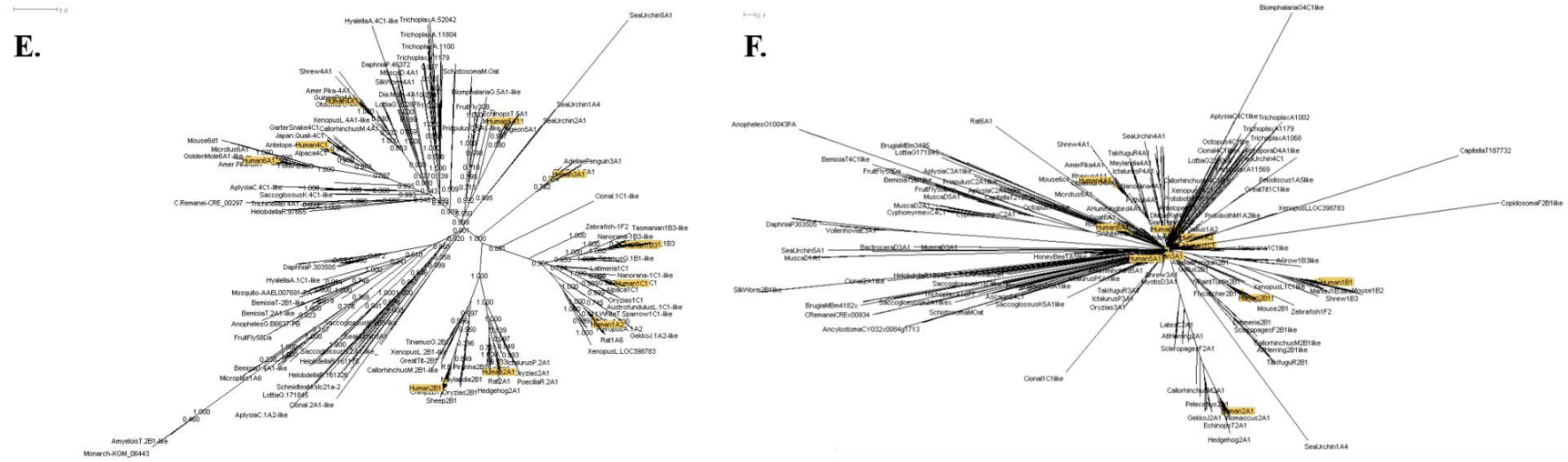

Figure 2: Phylogenetic Trees Constructed Using FastTree and MrBayes. Multiple sequence alignment of all 1264 sequences were created using (A-B) Clustal Omega, (C-D) MAFFT, and (E-F) QuickProbs and submitted to (A, C, E) FastTree and (B, D, F) MrBayes for phylogenetic tree construction. All 11 OATPs from *Homo sapiens* are highlighted in yellow.

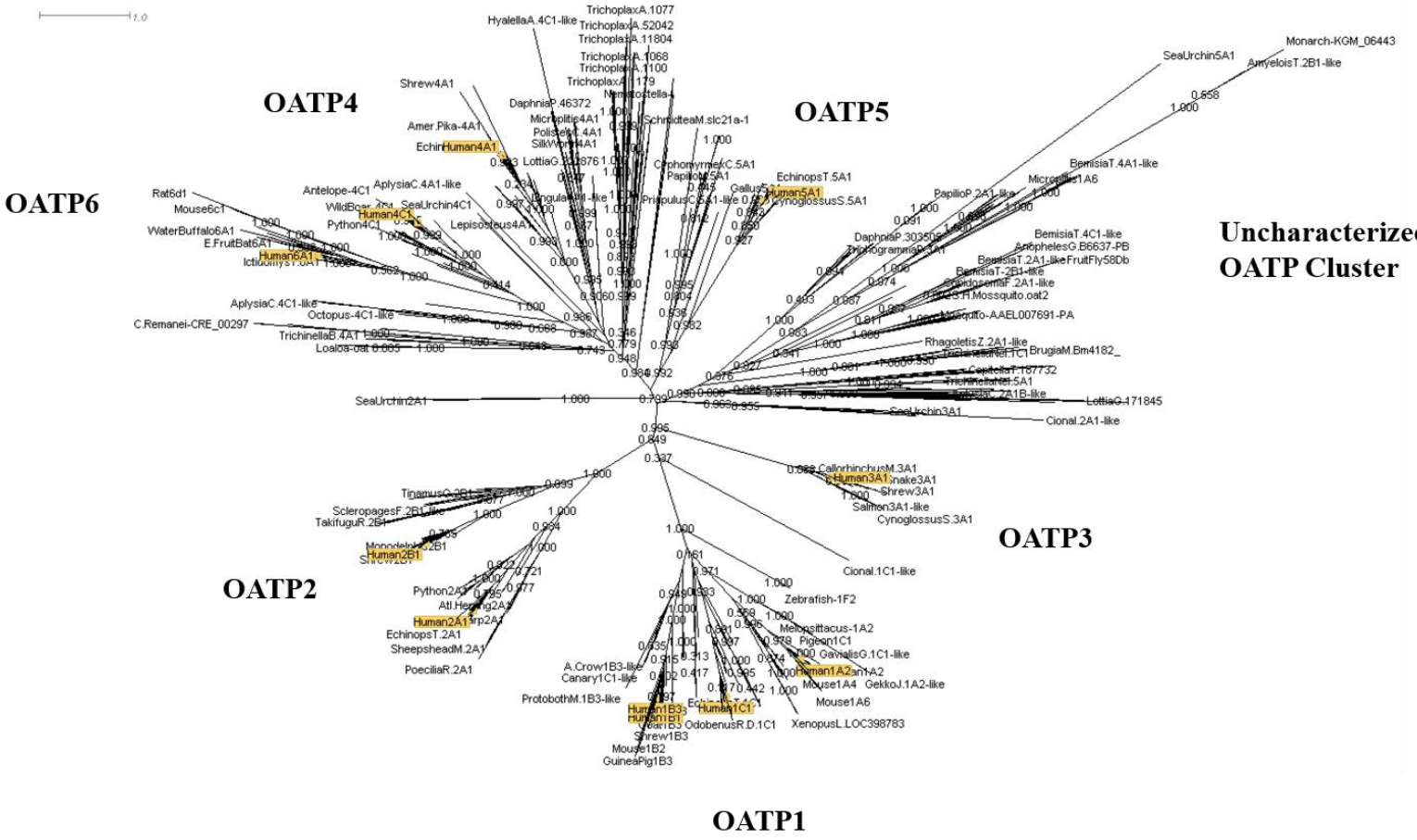

Figure 3: OATP Families Form Clusters in Phylogenetic Trees. In each of the phylogenetic trees constructed using FastTree, the six Oatp families form clusters with what looks to be a seventh family emerging labeled here as 'Uncharacterized OATP Cluster'. The tree depicted is a circular phylogram constructed using the Clustal Omega multiple sequence alignment and FastTree 2.0.

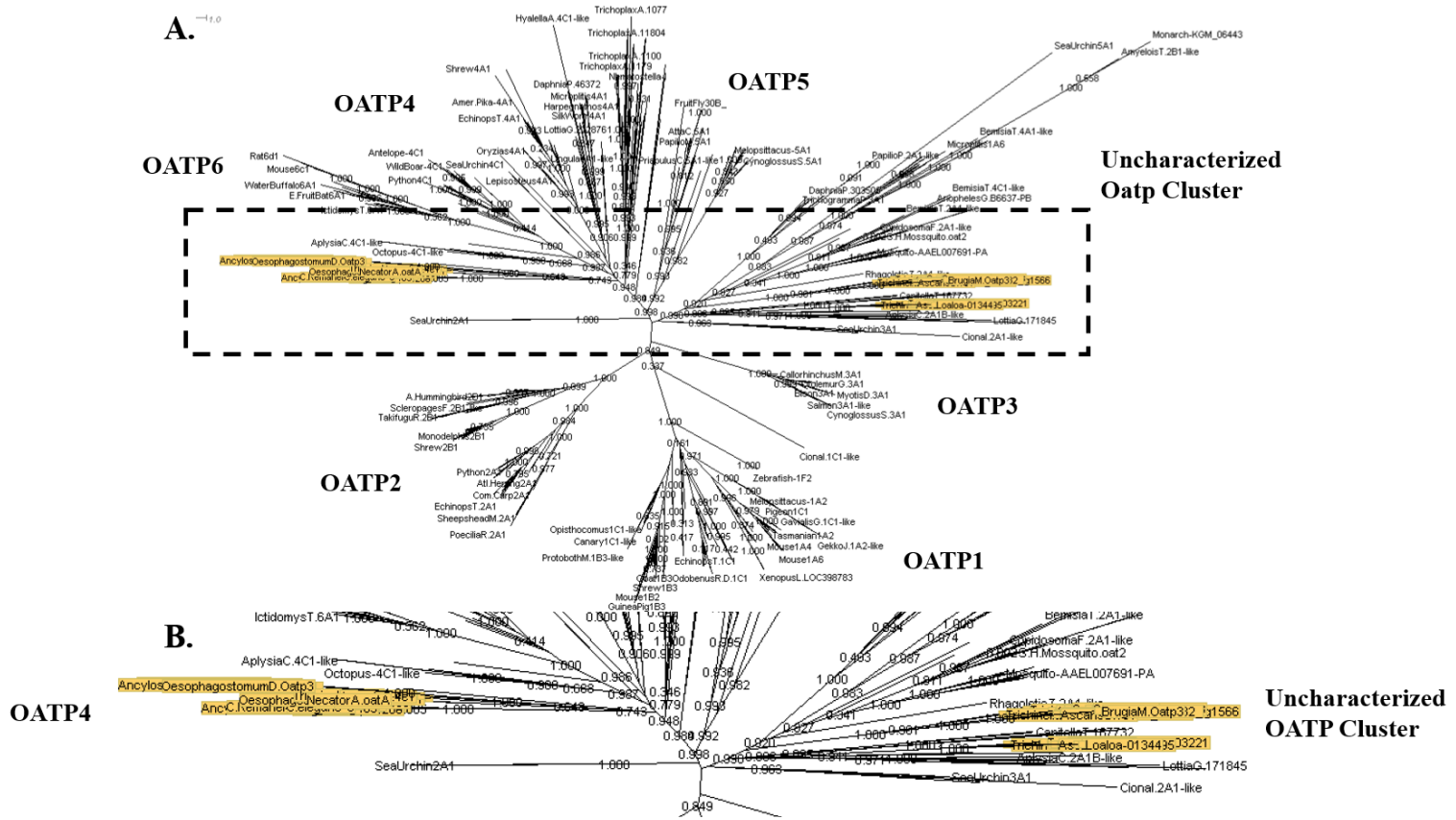

Figure 4: Phylum Nematoda Branches within Two Oatp Clusters in Phylogram. All species of the phylum Nematoda are highlighted in the FastTree phylogram constructed using the Clustal Omega multiple sequence alignment (A) illustrating the presence of proteins from two Oatp clusters within nematodes, the Oatp4 and the Uncharacterized Oatp cluster (B).

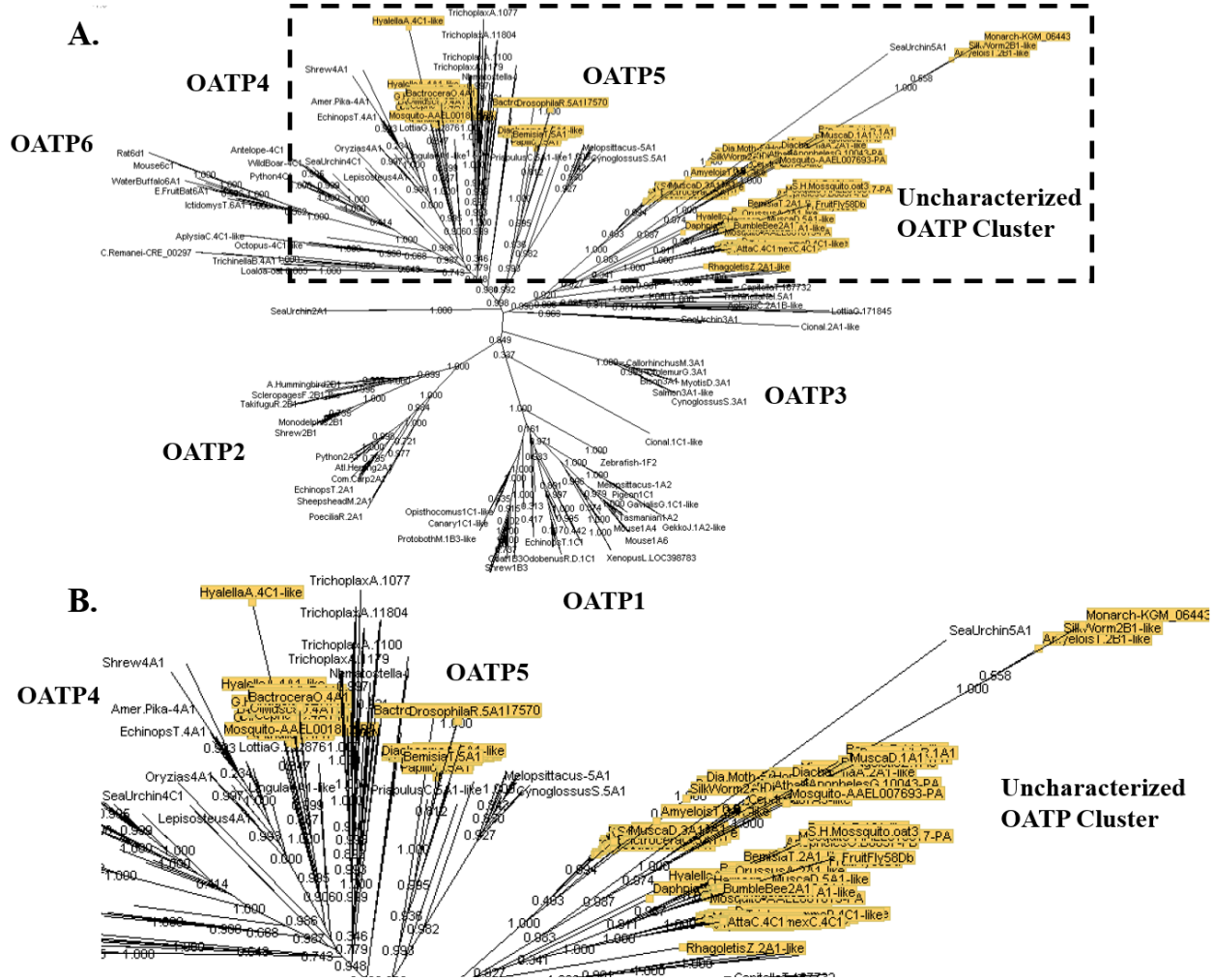

Figure 5: Phylum Arthropoda Branches within Three Oatp Clusters in Phylogram. All species of the phylum Arthropoda are highlighted (A) within the FastTree phylogram constructed using the Clustal Omega multiple sequence alignment. Zoomed in on the outlined area (B), visible are all Arthropoda branching within three Oatp clusters; Oatp4, Oatp5 and the Uncharacterized Oatp clusters.

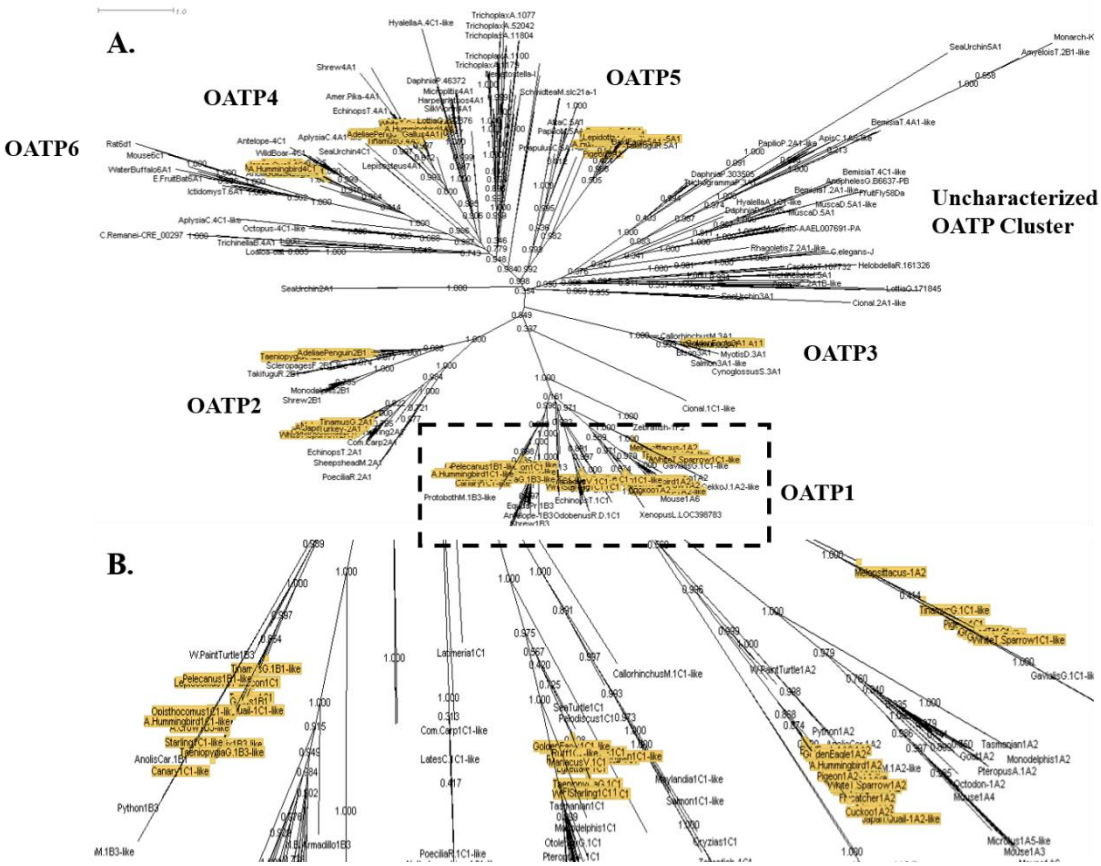

Figure 6: Neornithes are Present in All Oatp Familes. All species of the class Aves are highlighted in the FastTree phylogram created using the Clustal Omega multiple sequence alignment (A). Species from this class can be found in nearly all Oatp Clusters. Of interest is the species representation in the Oatp1 family (B). All but two species of class Aves included in these studies possess an Oatp1c1 and only seven species have an Oatp of the Oatp1b subfamily.

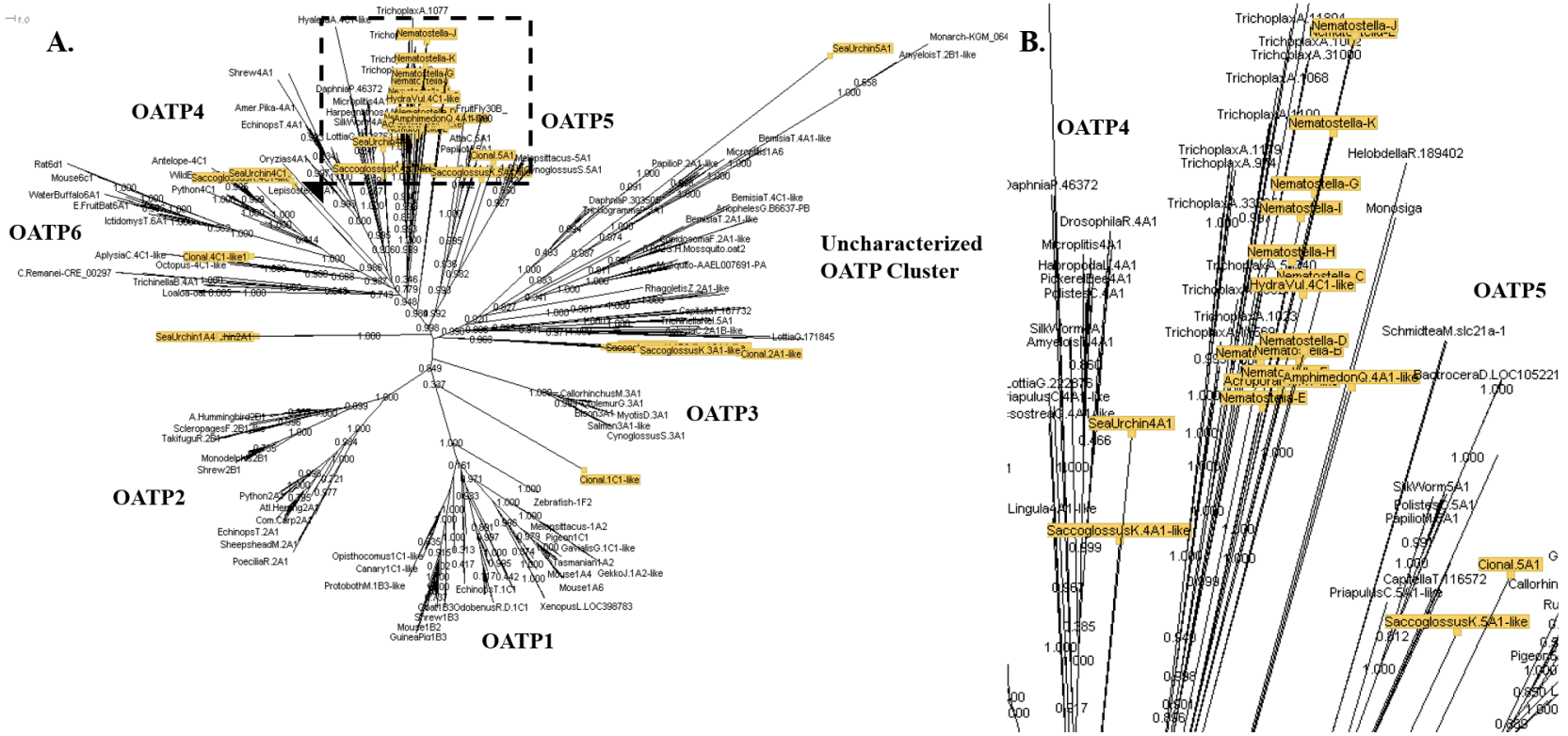

Figure 7: Early Evolution of Oatps. Starting with *Nematostella vectensis*, the evolution of organisms was traced to discover the transition from species with multiple closely related Oatps to species with more disparate Oatp sequences. All Oatp sequences possessed by *N. vectensis* where highlighted and nodes where counted to reveal *Amphimedon queenslandica*, *Acropora digitifera* and *Hydra vulgaris* as the closest branching organisms to *N. vectensis* with Sea Urchin (*Strongylocentrotus purpuratus*), *Saccoglossus kowalevskii*, and *Ciona intestinalis* the next closest organisms to branch (A). A closer look at the outlined area (B) depicts the

organisms previously mentioned and their close proximity to *N. vectensis*. The phylogram depicted was constructed using FastTree 2.0 and the Clustal Omega multiple sequence alignment.

Chapter 3

Comprehensive discussion, conclusions and future directions

Oatp Evolution

The overall studies presented here were designed to help elucidate the evolved biological function of Oatps. To achieve this, the evolutionary history of the entire Oatp family was constructed and transport inhibition studies against Oatp1c1-mediated uptake where conducted.

Oatps/OATPs are members of the SLC family of transporters and are evolutionarily conserved among bilaterians [Höglund et al., 2011]. Presumably the first Oatp, however, appears in the choanoflagellate *M. brevicollis*, the closest unicellular relatives to metazoans. Oatps are also found in other primitive metazoans including *T. adhaerens* and *N. vectensis*. *T. adhaerens* has the simplest body organization of all living metazoans and *N. vectensis* is the most primitive animal with specialized cell types. Because these simple organisms possess integral membrane transporters such as Oatps, an effort was made to reconstruct the evolutionary history of the Oatp family.

Data presented here demonstrates Oatps/OATPs present in metazoans likely evolved from a gene present in the last common ancestor of choanoflagellates and metazoans some 600+ million years ago. This is evidenced by the Oatp gene found in the genome of *M. brevicollis* and data showing choanoflagellates diverged before the origin of metazoans [King et al., 2008]. The Oatp sequence present in *M. brevicollis* is much smaller than the OATPs present in *H. sapiens* and in other metazoans, only 402 amino acids compared to the query sequence OATP4A1 of length 722 amino acids. This data, combined with data showing MFS members possess a two-fold symmetry, implicates the

12 TMD protein we see in metazoans today is the result of an intragenic duplication event(s) early in metazoan evolution [Saier, 2003].

The Oatp family is exclusive to *M. brevicollis* and to metazoans. Even though *M. brevicollis* is a single celled organism, the genome of *M. brevicollis* is complex with an estimated 9,196 genes, some having known functions in cell signaling and adhesion in higher metazoans [King et al., 2008]. This suggests the last common ancestor of choanoflagellates and metazoans likely possessed genes necessary for multicellularity [King et al., 2008]. It is possible *M. brevicollis* uses these proteins to facilitate environmental interactions as their functions in multicellular organisms are not needed in *M. brevicollis* [King et al., 2008].

Currently, it is unclear what purpose the Oatp transporter has in this single celled choanoflagellate. Possibly the gene encoding the Oatp protein differentially diversified along the choanoflagellate and the metazoan lineages resulting in altered functions within both lineages. The same concept of proteins having different functions in choanoflagellates and metazoans, as seen in the cell signaling and adhesion proteins, could also apply to Oatps. The genomes of some primitive metazoans including *A. queenslandica*, *T. adhaerens* and *N. vectensis* have recently been sequenced [Putnam et al., 2007; Srivastava et al., 2008 and 2010]. Further studies involving culturing *M. brevicollis*, *T. adhaerens* and *N. vectensis* for Oatp characterization may help elucidate the evolved physiological function of Oatps/OATPs.

Oatp/OATP Active Site Structure

Oatps/OATPs are bidirectional membrane transporters able to bind and translocate multiple unrelated amphipathic substrates including hormones and their conjugates, statins and anticancer agents. Multiple Oatps/OATPs have demonstrated atypical kinetic profiles suggestive of an active site containing more than one substrate binding site including Oatp1a4, OATP1B1, OATP1B3, Oatp1c1, OATP2B1 and OATP4C1 [Gui et al., 2008; Sugiyama et al., 2002; Tamai et al., 2001; Toyhama et al., 2004; Westholm et al., 2009a; Yamaguchi et al., 2010]. Oatps/OATPs are able to accept such a diverse range of substrates indicating they likely contain flexible active sites, or possibly multiple binding sites, capable of interacting with various steric surfaces.

Previous studies of Oatp1c1 have shown biphasic uptake curves for both T4 and E_2-17β-G as well as competitive inhibition between T4 and E_2-17β-G [Toyhama et al., 2004; Westholm et al., 2009]. Oatp1c1 was concluded to contained two substrate binding sites and T4 and E_2-17β-G shared the same binding sites but with differing affinities [Toyhama et al., 2004; Westholm et al., 2009a]. Research completed by the Rumbley Laboratory have aimed to characterize the high affinity T4 uptake site in Oatp1c1 using multiple different inhibitors (Table 1). The research completed here was aimed to characterize the E_2-17β-G binding site in Oatp1c1 using a subset of the same inhibitors used against the uptake of T4. This was to help elucidate the active site structure of Oatp1c1 as well as give insight into whether Oatp1c1 contains multiple substrate binding sites or one large substrate binding site. The data presented here along with IC_{50} values determined previously against the Oatp1c1-mediated uptake of T4 (Table 1), is suggestive of Oatp1c1 containing one large substrate binding site instead of two.

CYPs are xenobiotic metabolizing enzymes that exhibit atypical kinetics and have large, flexible binding sites capable of binding substrates of all different sizes, shapes and polarities [Li and Poulos, 2004]. CYP3A4, specifically, is capable of metabolizing almost 50% of drugs in use today ranging in molecular weights from 151 to 1203 grams per mole [Ekroos and Sjögren, 2006; Kapelyukh et al., 2008; Korzekwa, 2014]. At first, CYP3A4 was thought to contain multiple substrate binding sites due to differing K_i and K_m values for a given substrate [Hosea et al., 2000; Lin et al., 2001]. Research has since shown CYP3A4 possesses one large, flexible active site able to bind multiple substrate molecules simultaneously and the active site of CYP3A4 is capable of dramatic conformational shifts upon ligand binding [Dabrowski et al., 2002; Ekroos and Sjögren, 2006; Kapelyukh et al., 2008; Obach et al., 2006; Torimoto et al., 2003].

Inhibition studies against CYP3A4 substrate metabolism demonstrated IC_{50} values for each inhibitor was substrate dependent [Obach et al., 2006]. This data is consistent with the preliminary IC_{50} inhibitor screens presented here against Oatp1c1-mediated E_2-17β-G uptake. Almost all of the preliminary IC_{50} values presented in Table 1 are dissimilar when compared to uptake of T4. This indicates each of the inhibitors tested are interacting with the Oatp1c1 active site differently depending on the other substrate present. This is likely due to multiple substrate molecules simultaneously binding in the Oatp1c1 active site causing altered kinetics for each inhibitor tested or possibly a conformational shift taking place after a ligand molecule binds in the Oatp1c1 active site. However, the presence of a single flexible binding site does not explain the independently acting substrate recognition sites seen in OATP2B1 nor the biphasic

kinetic uptake up various substrates by multiple Oatps/OATPs [Gui et al., 2008; Shirasaka et al., 2012 and 2014; Sugiyama et al., 2002; Tamai et al., 2001; Toyhama et al., 2004; Westholm et al., 2009a; Yamaguchi et al., 2010]. Clearly, more research is needed to fully define the active site structure of Oatps/OATPs.

FUTURE DIRECTIONS

Immediate Future Directions

Investigations into the characterization of Oatp proteins within primitive organisms such as *M. brevicollis, N. vectensis* and *T. adhaerens* are needed to help elucidate the evolved physiological function of Oatps. Studying the environments of these primitive metazoans to learn how each of these organisms uptake nutrients and transport small molecules could also give insight into the possible roles transporter proteins played in early metazoan evolution. Also, performing a synteny analysis on Oatp genes within primitive metazoans could give insight into the functions these proteins serve in simpler organisms as well as how the genes encoding Oatp proteins have changed through the course of evolution.

To better define the active site structure of Oatp1c1, additional dose response assays are needed to determine the IC_{50} values for the inhibitors used here and in previous T4 inhibition assays. The characterization of substrate uptake by other OATPs, including OATP3A1, OATP4A1 and OATP6A1 have begun in the Rumbley Laboratory and will give further insight into the active site structure of Oatps/OATPs but further research is needed. However, the information gained from these studies will be

insufficient to determine the active site structure of Oatp1c1 so a crystal structure is needed.

OATP Expression in Cancer

Recent studies have demonstrated some OATPs have an altered expression profile, either up- or downregulated, in certain types of cancers [Obaidat et al., 2012]. Also, some OATPs with a restricted expression profile, OATP1B1 and OATP1B3 for example, are found to have increased expression in cancers throughout the body including breast and colon cancers [Obaidat et al., 2012]. This indicates OATPs could play a significant role in the development, progression and treatment of various cancer types.

Two-thirds of breast cancers are estrogen-dependent and inadequate supply of estrogen to cancerous cells inhibits cell proliferation [Maeda et al., 2012; Nozawa et al., 2005; Pasquakinin et al., 1989]. E-3-S is one of the most important circulating estrogens but remains biologically inactive until E-3-S is converted to the active form, estradiol, inside the cell [Maeda et al., 2012; Nozawa et al., 2005; Pasquakinin et al., 1989]. With E-3-S a common substrate to all OATPs, combined with the increased need for estrogen hormones in cancerous cells, OATPs not surprisingly are up-regulated or over-expressed within breast cancer cells. Nozawa et al. found breast cancer cell growth was increased in the presence of estrone or E-3-S in a dose-dependent manner and OATP1B3 was implicated in aiding cell growth through the transport of E-3-S [Maeda et al., 2010; Nozawa et al., 2005]. Additionally, OATP1A2 expression was increased in malignant

breast cancer tissue and likely responsible for the uptake of estrone into breast carcinoma cells [Meyer zu Schwabedissen et al., 2008; Miki et al., 2006].

The need for estrogen in estrogen-dependent cancers stems from the association of estrogen hormone with many cell-signaling pathways. In the presence of excess estrogen, the cell is able to up-regulate pathways involved in positive proliferation contributing to the overall stimulation of cell growth and also up-regulate growth factors, growth receptors, and hormone biosynthetic enzymes [Frasor et al., 2003]. There is also down-regulation of genes due to estrogen presence in estrogen-dependent cancers including apoptosis factors and other transcription factors and co-regulators [Frasor et al., 2003]. In order to obtain a higher amount of estrogen precursors for continued proliferation breast cancer cells seemingly up-regulate OATPs. It is unknown if all OATPs play a similar role in other types of cancers or what the implications of OATP expression are on certain cancerous tissues. Once OATPs are characterized and their physiological roles are understood, these questions are better addressed.

Because OATPs likely play a role in the development, progression and treatment of various cancer types, OATPs can act as specific targets for the development of anticancer therapies and pharmaceuticals. The extent of OATP expression and the physiological role each OATP is playing in all cancers is unknown. With further research into OATP expression and transport characteristics, OATPs can possibly act as targets for specific anti-cancer therapies and treatments.

So far, the overall structure of OATPs is unknown, along with their transport mechanism and their evolved biological role. Fully understanding these characteristics of

OATPs can lead to OATP-specific drug development. If the active site structure and transport mechanism is known for a particular OATP, a pharmaceutical agent can be developed to specifically bind and subsequently target certain tissues where this OATP is expressed, leading to a more effective therapy. With growing evidence of OATPs role in the progression and development of multiple types of cancers, further characterization of OATPs is needed for the future development of specifically targeted anti-cancer therapies.

COMPREHENSIVE BIBLIOGRAPHY

Abramson J, Smirnova I, Kasho V, Verner G, Kaback HR, Iwata S. (2003) Structure and mechanism of the lactose permease of *Escherichia coli*. Science 301(5633): 610-615

Adachi H, Suzuki T, Abe M, Asano N, Mizutamari H, Tanemoto M, Nishio T, Onogawa T, Toyohara T, Kasai S, Satoh F, Suzuki M, Tokui T, Unno M, Shimosegawa T, Matsuno S, Ito S, Abe T. (2003) Molecular characterization of human and rat organic anion transporter OATP-D. American Journal of Physiology-Renal Physiology 285: F1188-F1197

Akanuma S, Hirose S, Tachikawa M, Hosoya K. (2013) Localization of organic anion transporting polypeptide (Oatp) 1a4 and Oatp1c1 at the rat blood-retinal barrier. Fluids and Barriers of the CNS 10(29): 1-7

Alkemade A, Friesema ECH, Kalsbeek A, Swaab DF, Visser TJ, Fliers E. (2011) Expression of thyroid hormone transporters in the human hypothalamus. The Journal of Clinical Endocrinology and Metabolism 96(6): E967-E971

Altschul SF and Lipman DJ. (1990) Protein database searches for multiple alignments. Proceedings of the National Academy of Sciences 87(14): 5509-5513

Anderson GW, Schoonover CM, Jones SA. (2003) Control of thyroid hormone action in the developing rat brain. Thyroid 13(11): 1039-1056

Battaglia E, Gollan J. (2001) A unique multifunctional transporter translocates estradiol-17β-glucuronide in rat liver microsomal vesicles. The Journal of Biological Chemistry 276(26): 23492-23498

Chang C, Pang KS, Swaan PW, Ekins S. (2005) Comparative pharmacophore modeling of organic anion transporting polypeptides: a meta-analysis of rat Oatp1a1 and human Oatp1b1. The Journal of Pharmacology and Experimental Therapeutics 314: 533-541

Crantz FR, Silva JE, Larsen PR. (1982) An analysis of the sources and quantity of 3,5,3'-triiodothyronine specifically bound to nuclear receptors in rat cerebral cortex and cerebellum. Endocrinology 110(2): 367-375

Dabrowski MJ, Schrag ML, Wienkers LC, Atkins WM. (2002) Pyrene.pyrene complexes at the active site of cytochrome P450 3A4: evidence for multiple substrate binding site. Journal of the American Chemical Society 124(40): 11866-11867

Dehal P et al. (2002) The draft genome of *Ciona intestinalis*: insights into chordate and vertebrate origins. Science 298(5601): 2157-2167

Drewes LR. (2000) Molecular architecture of the brain microvasculature: perspective on blood-brain transport. Journal of Molecular Neuroscience 16(2): 93-98

Ekroos M, Sjögren T. (2006) Structural basis for ligand promiscuity in cytochrome P450 3A4. Proceedings of the National Academy of Sciences U.S.A 103(37): 13682-13687

Engelhardt B, Sorokin L. (2009) The blood-brain and the blood-cerebrospinal fluid barriers: function and dysfunction. Seminars in Immunopathology 31: 497-511

Frasor J, Danes J, Komm B, Chang K, Lyttle CR, Katzenellenbogen B, (2003) Profiling of estrogen up- and down-regulated gene expression in human breast cancer cells: insights into gene networks and pathways underlying estrogenic control of proliferation and cell phenotype. Endocrinology 144(10): 4562-4574

Friesema EC, Grueters A, Biebermann H, Krude H, von Moers A, Reeser M, Barrett TG, Mancilla EE, Svensson J, Kester MH, Kuiper GG, Balkassmi S, Uitterlinden AG, Koehrle J, Rodien P, Halestrap AP, Visser TJ. (2004) Association between mutations in a thyroid hormone transporter and severe x-linked psychomotor retardation. Lancet 364(9443): 1435-1437

Friesema EC, Jansen J, Milici C, Visser TJ. (2005) Thyroid hormone transporters. Vitamins and Hormones 70: 137-167

Friesema EC, Kuiper GG, Jansen J, Visser TJ, Kester MH. (2006) Thyroid hormone transport by the human monocarboxylate transporter 8 and its rate-limiting role in intracellular metabolism. Molecular Endocrinology 20(11): 2761-2772

Fujiwara K, Adachi H, Nishio T, Unno M, Tokui T, Okabe M, Onogawa T, Suzuki T, Asano N, Tanemoto M, Seki M, Shiiba K, Suzuki M, Kondo Y, Nunoki K, Shimosegawa T, Iinuma K, Ito S, Matsuno S, Abe T. (2001) Identification of thyroid hormone transporters in humans: different molecules are involved in a tissue-specific manner. Endocrinology 142(5): 2005-2012

Gabaldón T. (2007) Evolution of proteins and proteomes: a phylogenetics approach. Evolutionary Bioinformatics Online 1: 51-61

Gao B, Hagenbuch B, Kullak-Ublick GA, Benke D, Aguzzi A, Meier P. (2000) Organic anion-transporting polypeptides mediate transport of opioid peptides across blood-brain barrier. The Journal of Pharmacology and Experimental Therapeutics 294(1): 73-79

Gao B, Huber RD, Wenzel A, Vavricka SR, Ismair MG, Remé C, Meier PJ. (2005) Localization of organic anion transporting polypeptides in the rat and human ciliary body epithelium. Experimental Eye Research. 80(1): 61-72

Gao B, Stieger B, Noé B, Fritschy JM, Meier P. (1999) Localization of the organic anion transporting polypeptide 2 (Oatp2) in capillary endothelium and choroid plexus epithelial of rat brain. The Journal of Histochemistry and Cytochemistry 47(10): 1255-1263

Gudyś A and Deorowicz S. (2014) QuickProbs—a fast multiple sequence alignment algorithm designed for graphics processors. PLoS One 9(2): e88901

Gui C, Miao Y, Thompson L, Wahlgren B, Mock M, Stieger B, and Hagenbuch B. (2008) Effect of pregnane x receptor ligands on transport mediated by human OATP1B1 and OATP1B3. European Journal of Pharmacology 584(1): 57-65

Hagenbuch B, Meier PJ. (2003) The superfamily of organic anion transporting polypeptides. Biochimica et Biophysica Acta 1609(1): 1-18

Hagenbuch B, Meier PJ. (2004) Organic anion transporting polypeptides of the OATP/*SLC21* family: phylogenetic classification as OATP/*SLCO* superfamily, new nomenclature and molecular/functional properties. Pflugers Arch-European Journal of Physiology 447(5): 653-665

Hagenbuch B, Steiger B. (2013) The SLCO (former SLC21) superfamily of transporters. Molecular Aspects of Medicine 34: 396-412
Hänggi E, Grundschober AF, Leuthold S, Meier PJ, St-Pierre MV. Functional analysis of the extracellular cysteine residues in the human organic anion transporting polypeptide, OATP2B1. Molecular Pharmacology 70(3): 806-817
Hedlund E, Gustafsson JA, and Warner M. (2001) Cytochrome P450 in the brain: a review. Current Drug Metabolism 2(3): 245-263
Heuer H. (2007) The importance of the thyroid hormone transporters for brain development and function. Best Practice & Research. Clinical Endocrinology & Metabolism 21(2): 265-276
Höglund PJ, Nordström KJ, Schiöth HB and Fredriksson R. (2011) The solute carrier families have a remarkably long evolutionary history with the majority of the human families present before divergence of Bilaterian species. Molecular Biology and Evolution 28(4): 1531-1541
Hosea NA, Miller GP, Guengerich FP. (2000) Elucidation of distinct ligand binding sites for cytochrome P450 3A4. Biochemistry 39(20): 5929-5939
Huang Y, Lemieux MJ, Song J, Auer M, Wang DN. (2003) Structure and mechanism of the glycerol-3-phosphate transporter from *Escherichia coli*. Science 301: 616-620
Huber RD, Gao B, Pfändler MAS, Zhang-Fu W, Leuthold S, Hagenbuch B, Folkers G, Meier PJ, Stieger B. (2007) Characterization of two splice variants of human organic anion transporting polypeptide 3A1 isolated from human brain. American Journal of Physiology and Cell Physiology 292(2): C795-C806
Huelsenbeck JP, Larget B, Miller RE and Ronquist F. (2002) Potential applications and pitfalls of Bayesian inference of phylogeny. Systematic Biology 51(5): 673-688
Huson DH and Scornavacca C. (2012) Dendroscope 3: an interactive tool for rooted phylogenetic trees and netwroks. Systematic Biology 61(6): 1061-1067
Hvorup RN, Saier MH Jr. (2002) Sequence similarity between the channel-forming domains of voltage-gated ion channel proteins and the c-terminal domains of secondary carriers of the major facilitator superfamily. Microbiology 148(Pt 12): 3760-3762
Jedlitschky G, Cassidy AJ, Sales M, Pratt N, Burchell B. (1999) Cloning and characterization of a novel human olfactory UDP-glucuronosyltransferase. The Biochemical Journal 340(Pt 3): 837-843
Kapelyukh Y, Paine MJI, Maréchal JD, Sutcliffe MJ, Wolf CR, Roberts GCK. (2008) Multiple substrate binding by Cytochrome P450 3A4: estimation of the number of bound substrate molecules. Drug Metabolism and Disposition 36(10): 2136-2144
Katoh K, Misawa K, Kuma K and Miyata T. (2002) MAFFT: a novel method for rapid multiple sequence alignment based on fast Fourier transform. Nucleic Acids Research 30(14): 3059-3066
King CD, Rios GR, Assouline JA, Tephly TR. (1999) Expression of UDP-glucuronosyltransferases (UGTs) 2B7 and 1A6 in the human brain and

identification of 5-hydroxytryptamine as a substrate. Archives of Biochemistry and Biophysics 365(1): 156-162
King CD, Rios GR, Green MD, Tephly TR. (2000) UDP-glucuronosyltransferases. Current Drug Metabolism 1(2): 143-161
King N, et al. (2008) The genome of the choanoflagellate *Monosiga brevicollis* and the origin of metazoans. Nature 451(7180): 783-788
König J, Cui Y, Nies AT, Keppler D. (2000) Localization and genomic organization of a new hepatocellular organic anion transporting polypeptide. The Journal of Biological Chemistry 275(30): 23161-23168
Korzekwa K. (2014) Enzyme kinetics of oxidative metabolism: cytochrome P450. Methods in Molecular Biology 1113: 149-166
Kusuhara H, He Z, Nagata Y, Nozaki Y, Ito T, Masuda H, Meier PJ, Abe T, Sugiyama Y. (2003) Expression and functional involvement of organic anion transporting polypeptide subtype 3 (Slc21a7) in rat choroid plexus. Pharmaceutical Research 20(5): 720-727
Kusuhara H, Sugiyama Y. (2004) Efflux transport systems for organic anions and cations at the blood-CSF barrier. Advanced Drug Delivery Reviews 56:1741-1763
Kusuhara H, Sugiyama Y. (2005) Active efflux across the blood-brain barrier: role of the solute carrier family. The Journal of the American Society for Experimental NeuroTherapeutics 2:73-85
Larkin MA, Blackshields G, Brown NP, Chenna R, McGettigan PA, McWilliam H, Valentin F, Wallace IM, Wilm A, Lopez R, Thompson JD, Gibson TJ and Higgins DG. (2007) Clustal W and Clustal X version 2.0. Bioinformatics 23(21): 2947-2948
Law CL, Maloney PC, Wang DN. (2008) Ins and outs of major facilitator superfamily antiporters. Annual Review of Microbiology 62: 289-305
Lee TK, Koh AS, Cui Z, Pierce RH, Ballatori N. (2003) N-glycosylation controls functional activity of oatp1, an organic anion transporter. American Journal of Physiology Gastrointestinal and Liver Physiology 285(2): G371-381
Lee YJ, Kusuhara H, Sugiyama Y. (2004) Do multidrug resistance-associated protein-1 and -2 play any role in the elimination and estradiol-17β-glucuronide and 2,4-dinitrophenyl-*s*-glutathione across the blood-cerebrospinal fluid barrier. Journal of Pharmaceutical Sciences 93: 99-107
Lefort V, Longueville JE, and Gascuel O. (2017) SMS: Smart model selection in PhyML. Molecular Biology and Evolution 34(9): 2422-2424
Li H, Poulos TL. (2004) Crystallization of cytochromes P450 and substrate-enzyme interactions. Current Topics in Medicinal Chemistry 4(16): 1789-1802
Li L, Lee TK, Meier PJ, Ballatori N. (1998) Identification of glutathione as a driving force and leukotriene C_4 as a substrate for Oatp1, the hepatic sinusoidal organic solute transporter. The Journal of Biological Chemistry 273(26): 16184-16191
Li L, Meier PJ, Ballatori N. (2000) Oatp2 mediates bidirectional organic solute transport: a role for intracellular glutathione. Molecular Pharmacology 58(2): 335-340
Lin Y, Lu P, Tang C, Mei Q, Sandig G, Rodrigues AD, Rushmore TH, Shou M. (2001)

Substrate inhibition kinetics for cytochrome P450-catalyzed reactions. Drug Metabolism and Disposition 29(4): 368-374
Long H, Li M and Fu H. (2016) Determination of optimal parameters of MAFFT program based on BALiBASE3.0 database. Springerplus 5(1): 736
Lui Y, Schmidt B, Maskell DL. (2010) MSAProbs: multiple sequence alignment based on pair hidden Markov models and partition function posterior probabilities. Bioinformatics 26(16): 1958-1964
Maddison WP and Maddison DR. (2017) Mesquite: a modular system for evolutionary analysis. Version 3.31 http://mesquiteproject.org
Maeda T. Irokawa M, Arakawa H, Kuraoka E, Nozawa T, Tateoka R, Itoh Y, Nakanishi T, Tamai I. (2010) Uptake transporter organic anion transporting polypeptide 1B3 contributes to the growth of estrogen-dependent breast cancer. Journal of Steroid Biochemistry and Molecular Biology 122(4): 180-185
Maranduba CM, Friesema EC, Kok F, Kester MH, Jansen J, Sertié AL, Passos-Bueno MR, Visser TJ. (2006) Decreased cellular uptake and metabolism in Allan-Herndon-Dudley syndrome (AHDS) due to a novel mutation in the mct8 thyroid hormone transporter. Journal of Medical Genetics 43(5): 457-460
Mayerl S, Müller J, Bauer R, Richert S, Kassmann CM, Darras VM, Buder K, Boelen A, Visser TJ, Heuer H. (2014) Transporters mct8 and Oatp1c1 maintain murine brain thyroid hormone homeostasis. The Journal of Clinical Investigation 124(5): 1987-1999
McLysaght A, Hokamp K and Wolfe KH. (2002) Extensive genomie duplication during early chordate evolution. Nature Genetics 31(2): 200-204
Meier-Abt F, Mokrab Y, Mizuguchi K. (2005) Organic anion transporting polypeptides of the OATP/*SLCO* superfamily: identification of new members in nonmammalian species, comparative modeling and a potential transport mode. The Journal of Membrane Biology 208: 213-227
Meyer zu Schwabedissen HE, tirona RG, Yip CS, Ho RH, Kim RM. (2008) Interplay between the Nuclear Receptor Pregnane X Receptor and the Uptake Transporter Organic Anion Transporter Polypeptide 1A2 Selectively Enhances Estrogen Effects in Breast Cancer. Cancer Res. 68(22): 9338-9347
Miki Y, Suzuki T, Kitada K, Yabuki N, Shibuya R, Moriya T, Ishida T, Ohuchi N, Blumberg B, Sasano H. (2006) Expression of the steroid and xenobiotic receptor and its possible target gene, organic anion transporting polypeptide-A, in human breast carcinoma. Cancer Research 66(1): 535-542
Müller J, Heuer H. (2014) Expression pattern of thyroid hormone transports in the postnatal mouse brain. Frontiers in Endocrinology 5(92): 1-7
Nishino JI, Suzuki H, Sugiyama D, Kitazawa T, Ito K, Hanano M, Sugiyama Y. (1999) Transepithelial transport of organic anions across the choroid plexus: possible involvement of organic anion transporter and multidrug resistance-associated protein. The Journal of Pharmacology and Experimental Therapeutics 290(1): 289-294
Nozawa T, Suzuki M, Yabuuchi H, Irokawa M, Tsuji A, Tamai I. (2005) Suppression of cell proliferation by inhibition of estrone-3-sulfate transporter in estrogen-

dependent breast cancer cells. Pharmaceutical Research 22(10): 1634-1641
Obach RS, Walsky RL, Venkatakrishnan K, Gaman EA, Houston JB, Tremaine M. (2006) The utility of in vitro Cytochrome P450 inhibition data in the prediction of drug-drug interactions. The Journal of Pharmacology and Experimental Therapeutics 316(1): 336-348
Ohtsuki S, Takizawa T, Takanaga H, Hori S, Hosoya KI, Terasaki T. (2004) Localization of organic anion transporting polypeptide 3 (Oatp3) in mouse brain parenchymal and capillary endothelial cells. Journal of Neurochemistry 90: 743-749
Page RDM. (2003) Introduction to inferring evolutionary relationships. Current Protocols in Bioinformatics 6.1.1-6.1.13
Pardridge WM. (2003) Molecular biology of the blood-brain barrier. Methods in Molecular Medicine 89: 385-399
Pasquakinin JR, Gelly C, Nguyen BL, Vella C. (1989) Importance of estrogen sulfates in breast cancer. Journal of Steroid Biochemistry 34(1-6): 155-163
Pizzagalli F, Hagenbuch B, Stieger B, Klenk U, Folkers G, Meier PJ. (2002) Identification of a novel human organic anion transporting polypeptide as a high affinity thyroxine transporter. Molecular Endocrinology 16(10): 2283-2296
Price MN, Dehal PS, and Arkin AP. (2010) FastTree 2 – approximately maximum-likelihood trees for large alignments. PLoS One 5(3): e9490
Putnam NH, Srivastava M, Hellsten U, Dirks B, Chapman J, Salamov A, Terry A, Shapiro H, Lindquist E, Kapitonov VV, Jurka J, Genikhovich G, Grigoriev IV, Lucas SM, Steele RE, Finnerty JR, Technau U, Martindale MQ and Rokhsar DS. (2007) Sea anemone genome reveals ancestral eumetazoan gene repertoire and genomic organization. Science 317(5834): 86-94
Rao VV, Dahlheimer JL, Bardgett ME, Snyder AZ, Finch RA, Sartorelli AC, Piwnica-Worms D. (1999) Choroid plexus epithelial expression of *mrd1* p glycoprotein and multidrug resistance-associated protein contribute to the blood-cerebrospinal-fluid drug-permiability barrier. Proceedings of the National Academy of Sciences 96: 3900-3905
Roberts LM, Woodford K, Zhou M, Black DS, Haggerty JE, Tate EH, Grindstaff KK, Mengesha W, Raman C, Zerangue N. (2008) Expression of the thyroid hormone transporters monocarboxylate transporter-8 (Slc16a2) and organic ion transporter-14 (Slco1c1) at the blood-brain barrier. Endocrinology 149(12): 6251-61
Ronquist F and Huelsenbeck JP. (2003) MrBayes 3: Bayesian phylogenetic inference under mixed models. Bioinformatics 19(12): 1572-1574
Ronquist F, Teslenko M, Van Der Mark P, Ayres DL, Darling A, Höhna S, Larget B, Liu L, Suchard MA and Huelsenbeck JP. (2012) MrBayes 3.2: Efficient Bayesian phylogenetic inference and model choice across a large model space. Systematic Biology 61(3): 539-542
Roth M, Obaidat A, Hagenbuch B. (2012) OATPs, OATs and OCTs: the organic anion and cation transporters of the SLCO and SLC22A gene superfamilies. British

Journal of Pharmacology 165: 1260-1287
Saier, MH Jr. (2003) Tracing pathways of transport protein evolution. Molecular Microbiology 48(5): 1145-1156
Satlin LM, Amin V, Wolkoff AW. (1997) Organic anion transporting polypeptide mediates organic anion/HCO_3^- exchange. The Journal of Biological Chemistry 272(42): 26340-26345
Schnell C, Shahmoradi A, Wichert SP, Mayerl S, Hagos Y, Heuer H, Hülsmann S. (2015) The multispecific thyroid hormone transporter OATP1C1 mediates cell-specific sulforhodamine 101-labeling of hippocampal astrocytes. Brain Structure & Function 220: 193–203
Schweizer U, Köhrle J. (2013) Function of thyroid hormone transporters in the central nervous system. Biochimica et Biophysica Acta 1830(7): 3965-3973
Shawahna R, Uchida Y, Declèves X, Ohtsuki S, Yousif S, Dauchy S, Jacob A, Chassoux F, Daumas-Dupport C, Couraud PO, Terasaki T, Scherrmann JM. Transcriptomic and quantitative proteomic analysis of transporters and drug metabolizing enzymes in freshly isolated human brain microvessels. Molecular Pharmaceutics 8(4): 1332-1341
Shirasaka Y, Mori T, Murata Y, Nakanishi T, Tamai I. (2014) Substrate- and dose-dependent drug interactions with grapefruit juice cause by multiple binding sites on OATP2B1. Pharmaceutical Research 31(8): 2035-2043
Shirasaka Y, Mori T, Shichiri M, Nakanishi T, Tamai I. (2012) Functional pleiotropy of organic anion transporting polypeptides OATP2B1due to multiple binding sites. Drug Metabolism and Pharmacokinetics 27(3): 360-364
Sievers F, Wilm A, Dineen D, Gibson TJ, Karplus K, Li W, Lopez R, McWilliam H, Remmert M, Söding J, Thompson JD and Higgins DG. (2011) Fast, scalable generation of high-quality protein multiple sequence alignments using Clustal Omega. Molecular Systems Biology 7: 539
Söding J. (2005) Protein homology detection by HMM-HMM comparison. Bioinformatics 21(7): 951-960
Srivastava M, et al. (2008) The *Trichoplax* genome and the nature of placozoans. Nature 454(7207): 955-960
Srivastava M, et al. (2010) The *Amphimedon queenslandica* genome and the evolution of animal complexity. Nature 466(7307): 720-726
Stevenson RE, Goodman HO, Schwartz CE, Simensen RJ, McLean WT Jr, Herndon CN. (1990) Allan-Herndon syndrome. I. clinical studies. American Journal of Human Genetics 47(3): 446-453
Strazielle N, Ghersi-Egea JF. (2000) Choroid plexus in the central nervous system: biology and physiopathology. Journal of Neuropathology and Experimental Neurology 59(7): 561-574
Sugiyama D, Kusuhara H, Lee YJ, Sugiyama Y. (2003a) Involvement of multidrug resistance associated protein 1 (Mrp1) in the efflux transport of 17β estradiol-d-17β-glucuronide ($E_2$17βG) across the blood-brain barrier. Pharmaceutical Research 20(9): 1394-1400
Sugiyama D, Kusuhara H, Shitara Y, Abe T, Meier PJ, Sekine T, Endou H, Suzuki H,

Sugiyama Y. (2001) Characterization of the efflux transport of 17β-estradiol-D-17β-glucuronide from the brain across the blood-brain barrier. The Journal of Pharmacology and Experimental Therapeutics 298(1): 316-322

Sugiyama D, Kusuhara H, Shitara Y, Abe T, Sugiyama Y. (2002) Effect of 17 beta-estradiol-d-17 beta-glucuronide on the rat organic anion transporting polypeptide 2-mediated transport differs depending on substrates. Drug Metabolism and Disposition 30(2): 220-223

Sugiyama D, Kusuhara H, Taniguchi H, Ishikawa S, Nozaki Y, Aburatani H, Sugiyama Y. (2003b) Functional characterization of rat brain-specific organic anion transporter (Oatp14) at the blood-brain barrier. The Journal of Biological Chemistry 278(44): 43489-43495

Takano T, Tian GF, Peng W, Lou N, Libionka W, Han X, Nedergaard M. (2006) Astrocyte-mediated control of cerebral blood flow. Nature Neuroscience 9(2): 260-267

Tamai I, Nezu JI, Uchino H, Sai Y, Oku A, Shimane M, Tsuji A. (2000) Molecular identification and characterization of novel members of the human organic anion transporter (OATP) family. Biochemical and Biophysical Research Communications 273: 251-260

Tamai I, Nozawa T, Koshida M, Nezu JI, Sai Y, Tsuji A. (2001) Functional characterization of human organic anion transporting polypeptide b (Oatp-b) in comparison with liver-specific Oatp-c. Pharmaceutical Research 18(9): 1262-1269

Tohyama K, Kusuhara H, Sugiyama Y. (2004) Involvement of Multispecific Organic Anion Transporter, Oatp14 (Slc21a14), in the Transport of Thyroxine across the Blood-Brain Barrier. Endocrinology 145(9): 4384-4391

Torimoto N, Ishii I, Hata M, Nakamura H, Imada H, Ariyoshi N, Ohmori S, Igarashi T, Kitada M. (2003) Direct interaction between substrates and endogenous steroids in the active site may change the activity of cytochrome P450 3A4. Biochemistry 42(51): 15068-15077

Tracy TS, Hummel MA. (2004) Modeling kinetic data from in vitro drug metabolism enzyme experiments. Drug Metabolism Reviews 36(2): 231-242

Trajkovic M, Visser TJ, Mittag J, Horn S, Lukas J, Darras VM, Raivich G, Bauer K, Heuer H. (2007) Abnormal thyroid hormone metabolism in mice lacking the monocarboxylate transporter 8. The Journal of Clinical Investigation 117(3): 627-635

Westholm DE, Salo DR, Viken KJ, Rumbley JN, Anderson GW. (2009a) The blood-brain barrier thyroxine transporter organic anion-transporting polypeptide 1c1 displays atypical transport kinetics. Endocrinology 150(11): 5153-5162.

Westholm DE, Stenehjem DD, Rumbley JN, Drewes LR, Anderson GW. (2009b) Competitive inhibition of organic anion transporting polypeptide 1c1-mediated thyroxine transport by the fenamate class of nonsteroidal anti-inflammatory drugs. Endocrinology 150(2): 1025-1032

Whelan S, Goldman N. (2001) A general empirical model of protein evolution derived from multiple protein families using a maximum-likelihood approach.

Molecular Biology and Evolution 18(5): 691-699
Wohlburg H, Lippoldt A. (2002) Tight junctions of the blood-brain barrier: development, composition and regulation. Vascular Pharmacology 28: 323-337
Wolka A, Huber J, Davis T. (2003) Pain and the blood-brain barrier: obstacles to drug delivery. Advanced Drug Delivery Reviews 55: 987-1006
Yamaguchi H, Sugie M, Okada M, Mikkaichi T, Toyohara T, Abe T, Goto J, Hishinuma T, Shimada M, Mano N. (2010) Transport of estrone 3-sulfate mediated by organic anion transporter OATP4C1: estrone 3-sulfate binds to the different recognition site for digoxin in OATP4C1. Drug Metabolism and Pharmacokinetics 25(3): 314-317
Yamanda KD, Tomii K and Katoh K. (2016) Application of the MAFFT sequence alignment program to large data-reexamination of the usefulness of chained guide trees. Bioinformatics 32(21): 3246-3251
Yarim M, Moro S, Huber R, Meier PJ, Kaseda C, Kashima T, Hagenbuch B, Folkers G. (2005) Application of qsar analysis to organic anion transporting polypeptide 1a5 (Oatp1a5) substrates. Bioorganic and Medicinal Chemistry 13:463-471
Yang Z and Rannala B. (2012) Molecular phylogenetics: principles and practice. Nature Reviews: Genetics 13(5): 303-314
Yin Y, He X, Szewczyk P, Nguyen T, Chang G. (2006) Structure of the multidrug transporter EmrD from *Escherichia coli*. Science 312: 741-744